ONTARIO RESEARCH FOUNDATION
SHERIDAN PARK RESEARCH COMMUNITY
MISSISSAUGA, ONTARIO, CANADA L5K 1B3 • (416) 822 4111 • TELEX 06 982311

REQ. NO. 9-9081-1

Final Report No. 67042-81

Development of Abrasion Resistant Glass-Ceramics

for CONTRACT REPORT NO. OSQ80-00197

Department of Energy, Mines & Resources
CANMET, Mineral Sciences Laboratories
555 Booth Street
Ottawa, Ontario

Work on this project was conducted under the auspices of the Canada Centre for Mineral and Energy Technology, Energy, Mines and Resources, Canada.

DSS File No. : 18SQ.23440-9-9081-1
DSS Contract Serial No.: OSQ80-00197

D. Nguyen
M. van Roode
Glass & Ceramics Division
Department of Metals, Glass and Ceramics

April 30, 1982.

100 pp

WE, THE ONTARIO RESEARCH FOUNDATION, STIPULATE THAT THIS DOCUMENT IS SUBJECT TO THE FOLLOWING TERMS AND CONDITIONS.

1 ANY PROPOSAL CONTAINED HEREIN WAS PREPARED FOR THE CONSIDERATION OF THE ADDRESSEE ONLY. ITS CONTENTS MAY NOT BE USED BY NOR DISCLOSED TO ANY OTHER PARTY WITHOUT OUR PRIOR WRITTEN CONSENT.
2 ANY TESTING, INSPECTION OR INVESTIGATION PERFORMED BY US WILL BE CONDUCTED IN ACCORDANCE WITH NORMAL PROFESSIONAL STANDARDS. NEITHER WE NOR OUR EMPLOYEES SHALL BE RESPONSIBLE FOR ANY LOSS OR DAMAGE RESULTING DIRECTLY OR INDIRECTLY FROM ANY DEFAULT, ERROR OR OMISSION.
3 ANY REPORT, PROPOSAL OR QUOTATION PREPARED BY US REFERS ONLY TO THE PARTICULAR MATERIAL, INSTRUMENT OR OTHER SUBJECT REFERRED TO IN IT. NO REPRESENTATION IS MADE THAT SIMILAR ARTICLES WILL BE OF LIKE QUALITY.
4 NO REPORT ISSUED BY US SHALL BE PUBLISHED IN WHOLE OR IN PART WITHOUT OUR PRIOR WRITTEN CONSENT.
5 OUR NAME SHALL NOT BE USED IN ANY WAY IN CONNECTION WITH THE SALE, OFFER OR ADVERTISEMENT OF ANY ARTICLE, PROCESS OR SERVICE.
6 WE RESERVE THE RIGHT NOT TO COMMENCE AND/OR CONTINUE ANY WORK UNTIL PAYMENT ARRANGEMENTS SATISFACTORY TO US ARE ESTABLISHED.

(a)

SUMMARY

Glass-ceramics were produced from glass compositions in the alumino-silicate, basalt and slag systems. The abrasion resistance and fracture toughness of selected glass and glass compositions were evaluated. By modification of the heat treatment schedule glass-ceramics with high abrasion resistance were prepared. It was found that relatively short nucleation times produce glass-ceramics with the best abrasion resistance.

ORF

TABLE OF CONTENTS

		Page
1.	INTRODUCTION	1
2.	OBJECTIVES	2
3.	BACKGROUND INFORMATION	2
4.	EXPERIMENTAL	2
	4.1 Starting Materials	2
	4.2 Sample Preparation	3
	4.3 Characterization of Glasses and Glass-Ceramics	3
	4.4 Nucleation and Crystallization	7
	4.5 Heat Treatment of the Glasses	7
	4.6 Development of the Abrasion Testing Apparatus	7
	4.7 Glass-Ceramic Specimens for Abrasion Tests	10
	4.8 Fracture Testing and Crack Inhibition	10
5.	RESULTS AND DISCUSSION	11
	5.1 Preparation	11
	5.2 Characterization of Glasses and Glass-Ceramics	12
	5.3 Nucleation and Crystallization Studies	12
	5.4 Heat Treatment Studies of the Glasses	18
	5.5 Abrasion Testing Results	18
	5.6 Fracture Testing and Crack Inhibition	27
6.	CONCLUSIONS AND RECOMMENDATIONS	38
7.	ACKNOWLEDGEMENTS	38
	APPENDICES:	
	APPENDIX A: Abrasion Resistant Glass-Ceramics-Literature Review	1A
	APPENDIX B: Abrasion Testing Results of Glasses	1B
	APPENDIX C: Abrasion Testing Results of Glass-Ceramics	1C

1. INTRODUCTION

Glass-ceramics, the products of the controlled devitrification of glasses, have recently become commercially important materials for consumer products, vacuum tube envelopes, telescope mirror blanks, radomes for the aerospace industry and protective coatings for metals. Their properties, such as high hardness and excellent mechanical strength, superior electrical insulating properties and good thermal stability make them attractive for a number of specialized engineering applications.

A major use for glass-ceramics is in the development of abrasion resistant materials. Already, these materials have found applications for pipe linings, grinding media and as components for lubrication systems.

The Department of Mines, Energy and Resources over the past two years has sponsored a program for the development of abrasion resistant materials at the Ontario Research Foundation. Phase I of this program (Development of Abrasion Resistant Ceramics - DSS File No. 18SQ.23440-9-9081, Contract Serial No. OSQ79-00140) focussed on an investigation of abrasion resistant ceramics with an emphasis on inherent crack inhibition based on structural transitions in silicates. Although it was found difficult to obtain dense specimen the results were encouraging enough to initiate Phase II of the program, a study of abrasion-resistant glass ceramics based on alumino-silicate, basalt and slag compositions.

This report deals with the selection and development of such compositions as well as with an evaluation of their abrasion resistance and inherent crack inhibition.

2. OBJECTIVES

The objectives of the program are:

(1) Development of new glass-ceramics which show abrasion resistance.

(2) Investigation of inherent crack inhibition in the new glass-ceramics.

(3) Measurement of the relative abrasion resistance of the glass-ceramics.

3. BACKGROUND INFORMATION

A literature review of abrasion resistant glass-ceramics is given in Appendix A. The results of the experimental work to be discussed in subsequent sections will be evaluated with reference to this literature survey.

4. EXPERIMENTAL

4.1 Starting Materials

Fifteen glass compositions based on the alumino-silicate, basalt and slag systems were formulated. The compositions are shown in Table 1 (wt.%) and Table 2 (mole %). High-purity chemicals were used as the raw materials. The blast-furnace slag composition (No.15) is listed in Table 3.

ORF

4.2. Sample Preparation

Ball Milling:

The chemicals were mixed and milled in ethanol and in porcelain ball-mill jars using a borundum medium. The jar was rotated at 0.87 times the critical speed for two hours.

Calcination:

The milled raw materials were dried in a drying oven to remove the ethanol. The samples were calcined at 600^{o}C overnight.

Melting and Casting:

The glasses were melted in clay crucibles at temperatures between 1450^{o}C and 1500^{o}C and soaked for two to four hours. The melts were cast into bars and were transferred to an annealing furnace at a predetermined annealing temperature.

4.3 Characterization of Glasses and Glass-Ceramics

The thermal expansion coefficients, the annealing temperatures and the dilatometric softening points of the glasses and the derived glass-ceramics were measured. These parameters were used to check the uniformity of the glasses from various batches and also to estimate the gradient heat treatment temperature ranges for different glass compositions.

ORF

TABLE 1: Chemical Compositions (wt.%) of the Glasses

Components	1	2	3	4	5	6	7	8	9	10	11	12	13	14
SiO_2	48.9	47	34	50	55	52	45	50	45	45	45	45	45	45
Al_2O_3	24.9	13	9.9	25	15	15	11	20	15	15	15	10	10	15
MgO	-	11	3.9	5	5	5	10	10	15	20	10	10	10	10
CaO	15.1	12	40.6	15	10	10	10	5	25	20	25	25	20	20
TiO_2	11.1	3.8	1.0	5	5	5	5	10	-	-	5	10	15	10
Fe_2O_3	-	7	2.2	-	-	2	13	-	-	-	-	-	-	-
ZnO	-	-	-	-	1	2	2	-	-	-	-	-	-	-
Na_2O	-	3	.3	-	5	5	2	3	-	-	-	-	-	-
MnO	-	2	3.6	-	1	1	-	-	-	-	-	-	-	-
K_2O	-	2	.3	-	3	3	2	2	-	-	-	-	-	-
BaO	-	-	2.3	-	-	-	-	-	-	-	-	-	-	-
S	-	-	1.9	-	-	-	-	-	-	-	-	-	-	-

ORF

TABLE 2: Chemical Compositions (Mole %) of the Glasses

Components	1	2	3	4	5	6	7	8	9	10	11	12	13	14
SiO_2	55.51	49.33	34.44	54.34	58.44	56.15	49.75	53.33	43.70	42.83	45.32	44.95	45.68	46.06
Al_2O_3	16.64	8.04	5.91	16.01	9.39	9.55	7.17	12.57	8.58	8.41	8.90	5.89	5.98	9.05
MgO	-	17.21	5.89	8.10	7.92	8.05	16.48	15.90	21.71	28.37	15.01	19.89	15.13	15.26
CaO	18.37	13.49	44.07	17.47	11.38	11.57	11.84	5.72	26.01	20.39	26.98	26.76	21.75	21.93
TiO_2	9.47	3.00	.76	4.09	4.00	4.06	4.16	8.02	-	-	3.78	7.51	11.45	7.70
Fe_2O_3	-	2.76	.84	-	-	.81	5.41	-	-	-	-	-	-	-
ZnO	-	-	-	-	.79	1.60	1.63	-	-	-	-	-	-	-
Na_2O	-	3.05	.29	-	5.15	5.24	2.15	3.10	-	-	-	-	-	-
MnO	-	1.78	3.09	-	.90	.91	-	-	-	-	-	-	-	-
K_2O	-	1.33	.19	-	2.03	2.06	1.41	1.36	-	-	-	-	-	-
BaO	-	-	.91	-	-	-	-	-	-	-	-	-	-	-
S	-	-	3.61	-	-	-	-	-	-	-	-	-	-	-

ORF

TABLE 3: Chemical Composition of Glass No. 15 (wt.%)

Blast Furnace Slag	56%
Sand	28%
Sodium Carbonate	4.8%
Sodium Sulphate	5.6%
Silica	4.5%
Alumina	1.1%

4.4 Nucleation and Crystallization

Nucleation and Crystallization temperatures of the glasses were identified using Differential Thermal Analysis (DTA), gradient heat treatment and X-ray diffraction analysis or laser light scattering.

4.5 Heat Treatment of the Glasses

The glasses were heat treated in a two-stage heating process using the predetermined nucleation and crystallization temperatures. Several different heat treatment schedules in time and temperature were applied. The heat treatment processes were conducted in an isothermal furnace (A4) and in a programable controlled furnace (Deltech 1).

4.6 Development of the Abrasion Testing Apparatus

A device to measure the abrasion based on ASTM 158-72 was designed and constructed. This set-up is shown schematically in Figure 1. A close-up of the abrasion testing system is shown in Figure 2. It consists of a pressure line, an inlet by which grits or sand are introduced, and an exhaust line to remove the grits during and after the experiment.

The operating parameters are pressure, weight of the grit and duration of the testing. Preliminary tests of the grit blaster were conducted to optimize the operating parameters. The operating conditions are:

- air pressure : 40 psi
- weight of grits : 35
- time of operation : 60 s

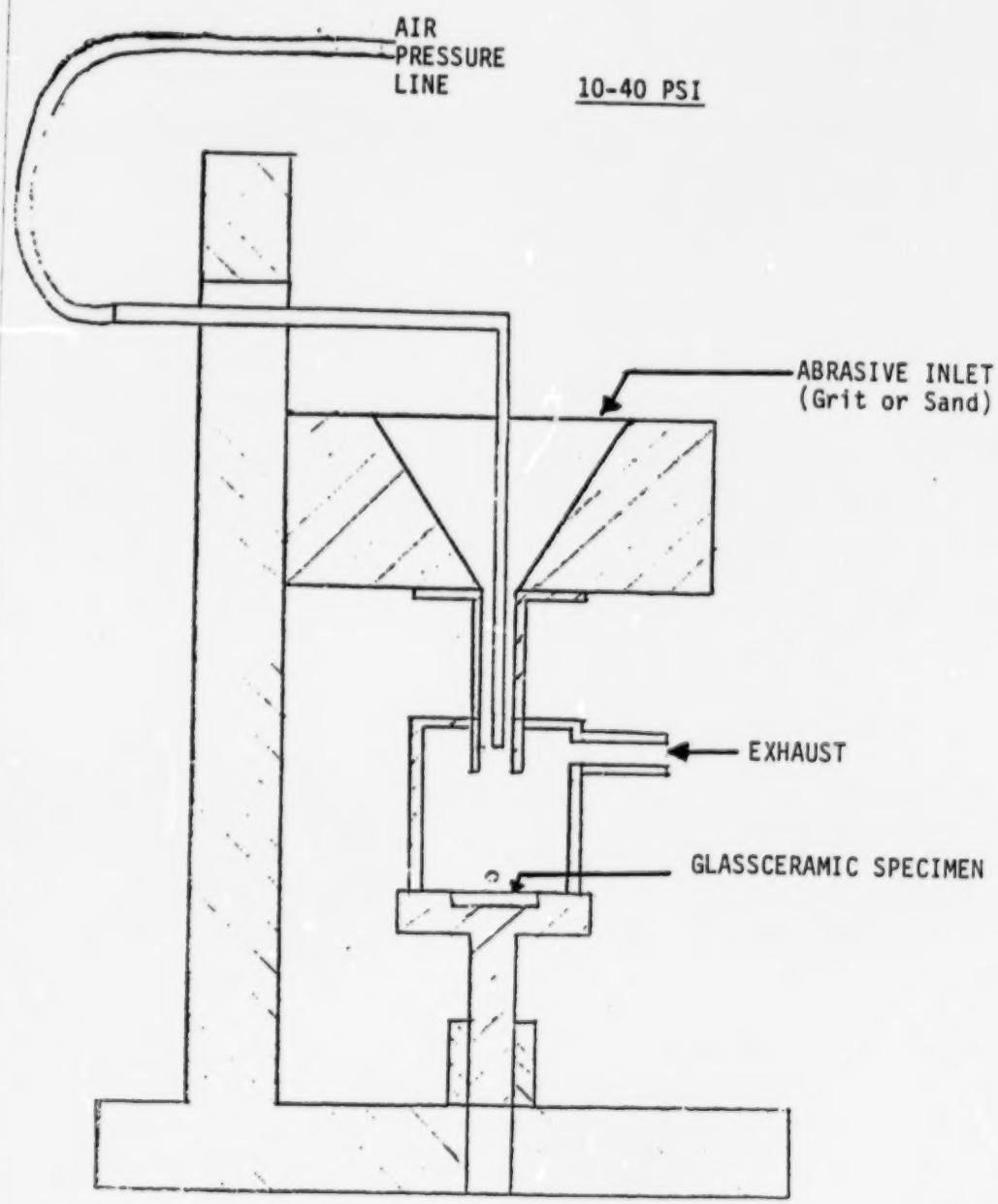

FIGURE 1: Sand/Grit Blaster
(Abrasion Testing Device)

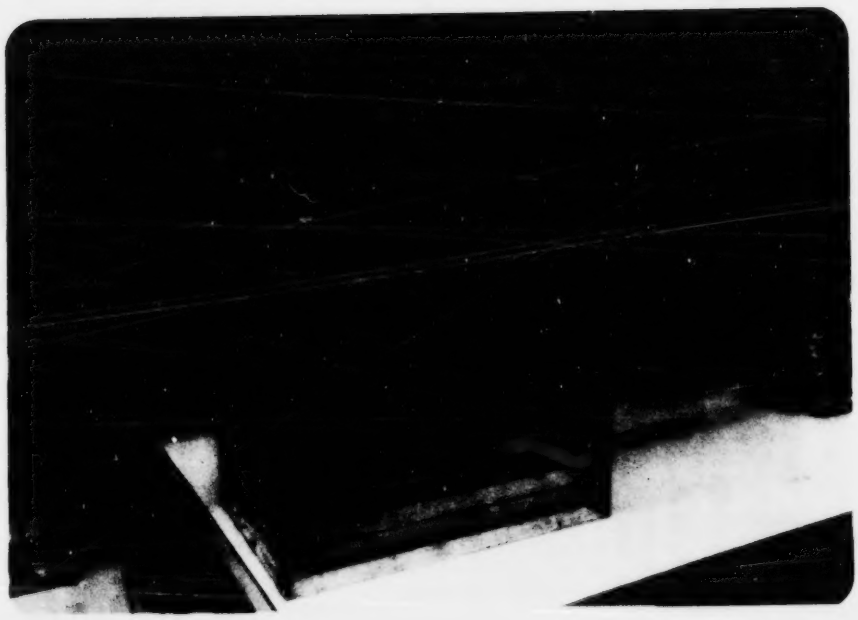

FIGURE 2: Sand/grit blaster for abrasion resistance measurements.

4.7 Glass and Glass-Ceramic Specimens for Abrasion Tests

The glasses and glass-ceramics were cut into rectangular bars (¼x½x1") and were polished with a series of silicon papers having grit sizes of 240, 320, 400 and 600. Subsequent polishing was carried out with a nylon cloth and alumina powder (particle size 5μm).

The abrasion tests were performed mostly in quadruplicate.

4.8 Fracture Testing and Crack Inhibition

Glass and glass-ceramic samples were also prepared for 4-point bending tests. Selected glass compositions were melted and poured into bars (¼x1x3½"). After annealing, these glass bars were heat treated in an isothermal furnace and were converted to fine-grained glass-ceramics.

The crystalline glass-ceramics were then fractured on a four-point bending jig with an Instron testing machine. The initial load was started at zero and the loading rate was about 0.05 cm/min. (0.02 in/min). The movement arm (separation of the adjacent support and loading edges) was 2.5 cm. The separation of the loading edges was 2 cm.

The fracture surface of the glass-ceramics were examined with the optical and Scanning Electron Microscope (SEM) to investigate the crack inhibition in the glass-ceramics.

ORF

5. RESULTS AND DISCUSSION

5.1 Preparation

The prepared glasses posses a variety of colours ranging from black to green as shown in Table 4.

TABLE 4: Glass Colours

Glass Compositions	Colour
2,6,7	Black
5,8,13,14	Brown
11,15	Yellowish Brown
12	Greenish Yellow
1,4	Yellow
9,10	Green

All glass melted easily at 1450^{o}C. Some of the glasses with a high silica content had high viscosities and were hard to pour. Glass No.3 was rejected since it appeared to have reacted with the clay crucible. The melting of glass No.15 was accompanied by the generation of many gas bubbles.

5.2 Characterization of Glasses and Glass-Ceramics

The thermal expansion coefficients, the annealing temperatures and the dilatometric softening points of glasses and glass-ceramics are shown in Tables 5 and 6.

The thermal expansion coefficients of the glasses range from 5.28 to 9.26×10^{-6} cm/cm/^{o}C while those of glass-ceramics range from 6.48 to 10.27×10^{-6} cm/cm/^{o}C. The dilatometric softening points of the glass-ceramics are much higher than those of the parent glasses. For several glass-ceramics, the softening point exceeds 1,000^{o}C. A typical thermal expansion curve of glass in shown in Figure 3.

5.3 Nucleation and Crystallization Studies

Nucleation and crystallization temperatures of the glasses were identified with the application of the following techniques:

- Differential Thermal Analysis (DTA). A DTA curve of glass No.2 is shown in Figure 4. This curve displayed an exothermic peak where crystallization occurred. The smaller peak corresponded to the annealing temperature of the glass.

- Gradient heat treatment, X-ray analysis or laser light scattering. These techniques were mainly employed to determine the nucleation and crystallization temperature range.

  The temperature range for nucleation and the minimum crystallization temperatures are given in Table 7.

TABLE 5: Coefficients of Thermal Expansion of the Glasses

Glass Composition	Thermal Expansion Coefficient (cm/cm/^{o}C) x^{-6}	Annealing Temperature (^{o}C)	Dilatometric Softening Point ^{o}C
1	5.33	780	835
2	7.57	670	710
3	-	-	-
4	5.28	780	820
5	7.82	700	760
6	6.45	680	730
7	5.16	700	740
8	7.99	720	780
9	6.88	770	815
10	7.96	780	820
11	9.26	750	800
12	6.49	750	820
13	7.02	770	830
14	6.25	775	830
15	8.20	720	775

ORF

TABLE 6: Coefficients of Thermal Expansion of the Glass-Ceramics

Sample No.	HEAT TREATMENT SCHEDULE		Dilatometric Softening Point	Thermal Expansion Coefficients
	Nucleation	Crystallization	(^{o}C)	(cm/cm/^{o}C x 10^{-6})
1	900^{o}C (24 hours)	1000^{o}C (24 hours)	>1091	6.60
2	900^{o}C (24 hours)	950^{o}C (24 hours)	>1050	7.39
5	900^{o}C (17 hours)	950^{o}C (24 hours)	951	8.17
6	800^{o}C (24 hours)	860^{o}C (24 hours)	750	7.76
7	850^{o}C (4 hours)	950^{o}C (24 hours)	>1050	8.23
8	850^{o}C (4 hours)	950^{o}C (24 hours)	975	7.54
13	900^{o}C (24 hours)	950^{o}C (24 hours)	>1050	6.48
14	850^{o}C (24 hours)	950^{o}C (24 hours)	>1075	7.21
15	850^{o}C (24 hours)	950^{o}C (24 hours)	>1080	10.27

ORF

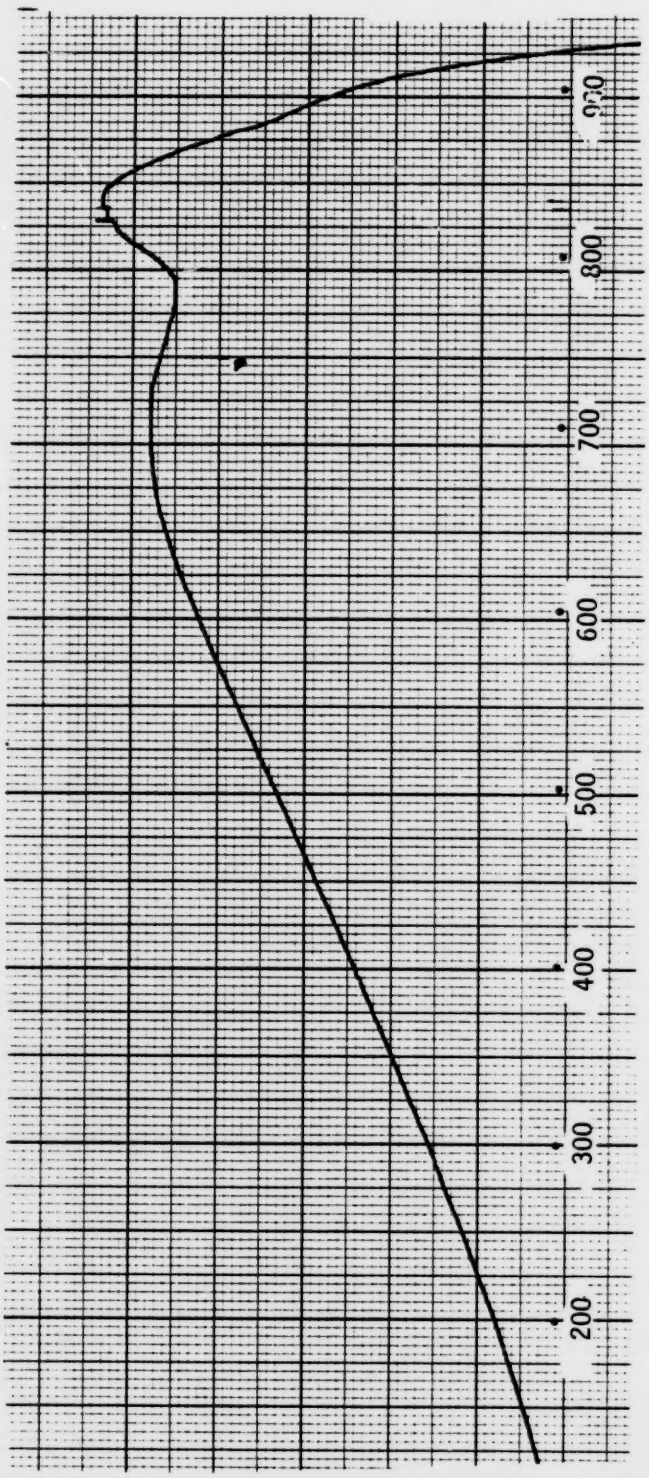

FIGURE 3: Thermal Expansion Curve of Glass No.2

TABLE 7: Nucleation and Crystallization Temperature of the Glasses

Glass Composition	Nucleation Temperature Range (°C)	Minimum Crystallization Temperature (°C)	Method of Detection
1	820 - 850	900	X-ray
2	720	740	X-ray & DTA
3	-	-	-
4	830 - 850	860	X-ray
5	780 - 850	860	X-ray & Laser
6	720 - 800	810	Laser
7	750 - 805	810	X-ray
8	860 - 900	905	X-ray
9	820 - 900	900	X-ray & DTA
10	930 - 935	935	X-ray & DTA
11	800 - 925	925	X-ray
12	800 - 900	900	X-ray
13	820 - 850	855	X-ray
14	825 - 830	830	X-ray
15	800 - 850	850	X-ray

ORF

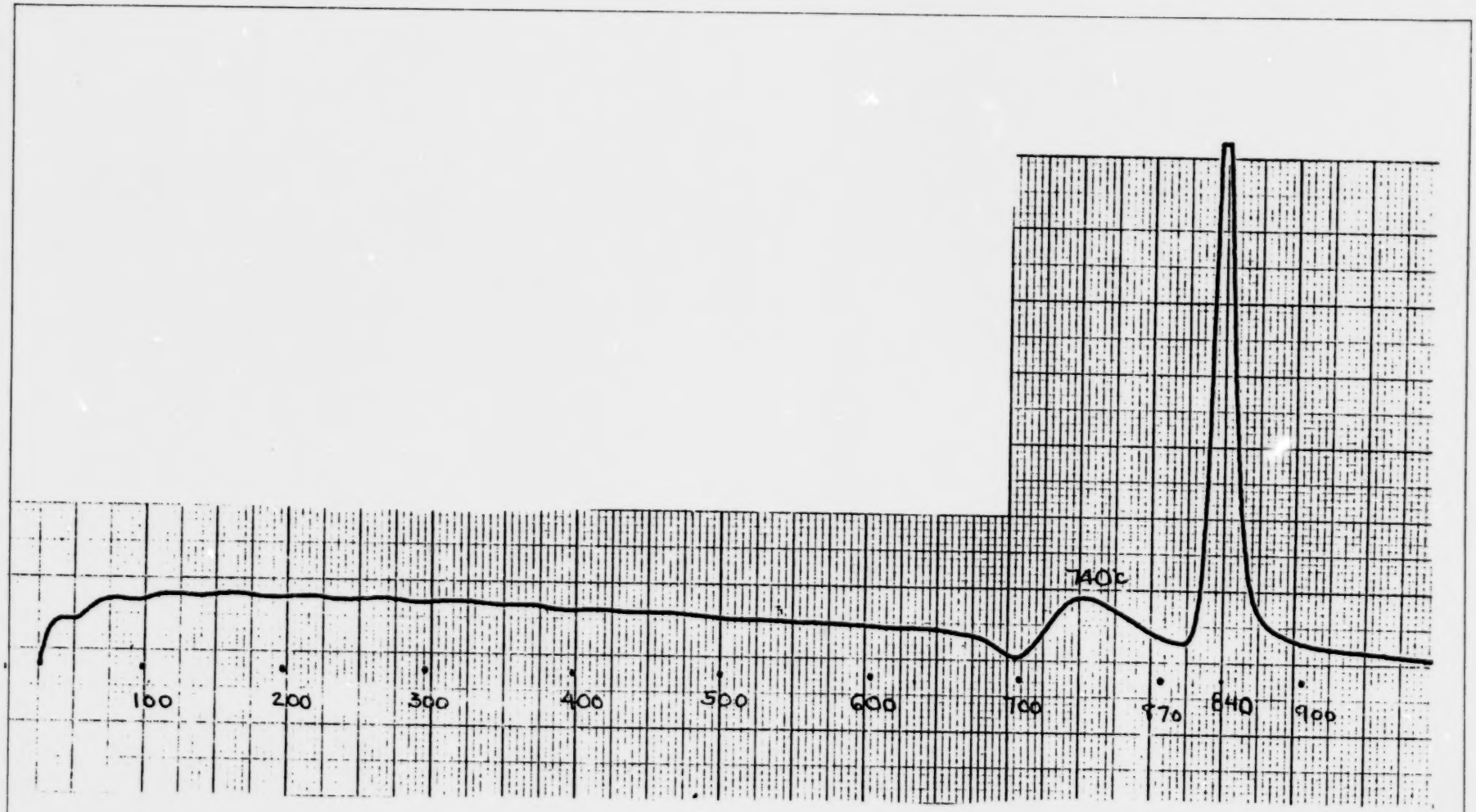

FIGURE 4: Differential Thermal Analysis of Glass #2

ORF

5.4 Heat Treatment of Glasses

The majority of the glasses were successfully heat treated to give fine-grained glass-ceramics. Exceptions were the glass compositions numbers 4,9,10,11 and 12. The various heat treatment programs have been summarized in Table 8. X-ray powder crystallography was used to identify the crystalline phases present in the heat treated glass-ceramics. The results are shown in Table 9. The major crystalline phase present are anorthite and diopside with minor quantities of Ti-containing phases for the compositions to which TiO_2 was added. The Minelbite glass-ceramics reported by Locsei (Appendix A, reference 20) which were derived from blast-furnace slag had a high diopside content. These glass-ceramics had reportedly a high mechanical strength, good chemical stability, and high wear resistance.

5.5 Abrasion Testing Results

The abrasion resistance of the glasses and derived glass-ceramics are illustrated in Table 10. A complete data set for the abrasion tests for glasses is given in Appendix B and for glass-ceramics subjected to various heat treatment schedules is given in Appendix C. Table 10 shows the average weight loss per unit area for the glasses and for the glass-ceramics with the highest abrasion resistance for each composition.

Since the ~~abrasion resistance~~ weight loss of the glass-ceramics is in all cases lower than that of the parent glasses it follows that the heat treatment substantially improves the resistance to wear of the compositions. The greatest proportional improvement was observed for composition 7 where the abrasion resistance of the original glass was improved more than four-fold after heat treatment.

ORF

TABLE 8: Heat Treatment Data

Glass No.	Nucleation		Crystallization		Results
	Time (Hrs.)	Temp. (^{o}C)	Time (Hrs.)	Temp. (^{o}C)	
1	6	840	24	950	White opaque hard
1	24	730	24	900	White opaque hard
1	12	860	24	960	White opaque hard
1	24	950	24	1050	White opaque hard
1	24	900	24	1000	Milky orange hard
2	24	730	24	900	Black, hard
2	12	800	24	830	Grey, hard
2	24	900	24	950	Hard, Silver Brown
2	4	850	24	950	Greenish Brown hard
5	17	900	24	950	Bluish colour hard
5	4	810	14	910	Bluish colour hard
5	19	750	24	850	White, hard
5	24	750	24	800	Brownish White hard
6	24	800	24	860	Green-grey hard
6	24	730	24	900	Green-grey hard
6	4	800	20	1000	Grey, hard
6	10	820	24	880	Grey, hard
7	24	730	24	900	Black, hard
7	12	800	24	830	Black, hard
7	4	800	24	830	Solid Black
7	24	800	12	950	Solid Black
7	24	900	24	950	Dark Greenish Brown, hard
8	12	850	24	950	Bluish, hard
8	27	800	65	900	Hard, blue
8	24	850	12	950	Hard, blue
8	24	850	24	950	Hard, blue
8	24	900	24	950	Hard, white
8	4	850	24	950	Hard, white
11	4	850	24	950	Greyish white
13	12	850	24	950	Light blue hard
13	24	850	24	950	Bluish grey
13	27	850	65	950	Navy bluish grey
13	24	900	24	950	White and blue
13	4	850	24	950	Milky white
14	24	850	24	950	Hard, grey
14	27	850	65	950	Greenish grey
14	24	900	24	950	Glass melted
15	24	850	24	950	Light grey

ORF

TABLE 8: Heat Treatment Data

Glass No.	Nucleation		Crystallization		Results
	Time (Hrs.)	Temp. (°C)	Time (Hrs.)	Temp. (°C)	
1	6	840	24	950	White opaque hard
1	24	730	24	900	White opaque hard
1	12	860	24	960	White opaque hard
1	24	950	24	1050	White opaque hard
1	24	900	24	1000	Milky orange hard
2	24	730	24	900	Black, hard
2	12	800	24	830	Grey, hard
2	24	900	24	950	Hard, Silver Brown
2	4	850	24	950	Greenish Brown hard
5	17	900	24	950	Bluish colour hard
5	4	810	14	910	Bluish colour hard
5	19	750	24	850	White, hard
5	24	750	24	800	Brownish White hard
6	24	800	24	860	Green-grey hard
6	24	730	24	900	Green-grey hard
6	4	800	20	1000	Grey, hard
6	10	820	24	880	Grey, hard
7	24	730	24	900	Black, hard
7	12	800	24	830	Black, hard
7	4	800	24	830	Solid Black
7	24	800	12	950	Solid Black
7	24	900	24	950	Dark Greenish Brown, hard
8	12	850	24	950	Bluish, hard
8	27	800	65	900	Hard, blue
8	24	850	12	950	Hard, blue
8	24	850	24	950	Hard, blue
8	24	900	24	950	Hard, white
8	4	850	24	950	Hard, white
11	4	850	24	950	Greyish white
13	12	850	24	950	Light blue hard
13	24	850	24	950	Bluish grey
13	27	850	65	950	Navy bluish grey
13	24	900	24	950	White and blue
13	4	850	24	950	Milky white
14	24	850	24	950	Hard, grey
14	27	850	65	950	Greenish grey
14	24	900	24	950	Glass melted
15	24	850	24	950	Light grey

ORF

TABLE 9: Phases Detected in the Glass-Ceramics with X-ray Powder Crystallography

Composition	Heat Treatment		Phases Present
	Nucleation	Crystallization	
1	950°C (24 hrs)	1050°C (24 hrs)	Anorthite ($CaAl_2SiO_8$) Pseudoanatase ($Al_4Ti_2SiO_{12}$) Aluminum Titanium Oxide (Al_2TiO_5)
2	900°C (24 hrs)	950°C (24 hrs)	Diopside ($CaMgSi_2O_6$) Kennedyite ($Fe_2MgTi_3O_{10}$)
5	900°C (17 hrs)	950°C (24 hrs)	Aluminum Magnesium Titanium Oxide ($MgAl_2Ti_3O_{10}$) Calcium Titanium Oxide ($CaTi_2O_5$)
6	820°C (10 hrs)	880°C (24 hrs)	Anorthite ($CaAl_2SiO_8$) Diopside ($CaMgSi_2O_6$)
7	850°C (4 hrs)	950°C (24 hrs)	Diopside ($CaMgSi_2O_6$)
8	900°C (24 hrs)	950°C (24 hrs)	Calcium Titanium Oxide ($CaTi_2O_5$) Aluminum Magnesium Titanium Oxide ($MgAl_2Ti_3O_{10}$)
13,14,15	850-900°C (24 hrs)	950°C (24 hrs)	Diopside ($CaMgSi_2O_6$) Anorthite ($CaAl_2Si_2O_8$) Wollastonite ($CaSiO_3$) Pyroxene ($CaAl_2SiO_6$)
15			also: Pseudoanatase ($Al_4Ti_2SiO_{12}$) Calcium Titanium Oxide $CaTi_2O_5$)

TABLE 10: Abrasion Tests on Glasses and Glass-Ceramics

Composition	Glass (Average Wt. Loss /unit area - $g.dm^{-2} \times 10^{-1}$)	Glass-Ceramic (Average Wt. Loss /unit area - $g.dm^{-2} \times 10^{-1}$)
1	6.8	3.6
2	8.8	4.2
5	10.8	4.5
6	-	4.0
7	10.5	2.5
8	7.4	5.8
12	8.6	-
13	8.2	3.8
14	8.0	3.0
15	10.1	4.5
High Density Al_2O_3	0.45	

Average Precision of Results: 5%

ORF

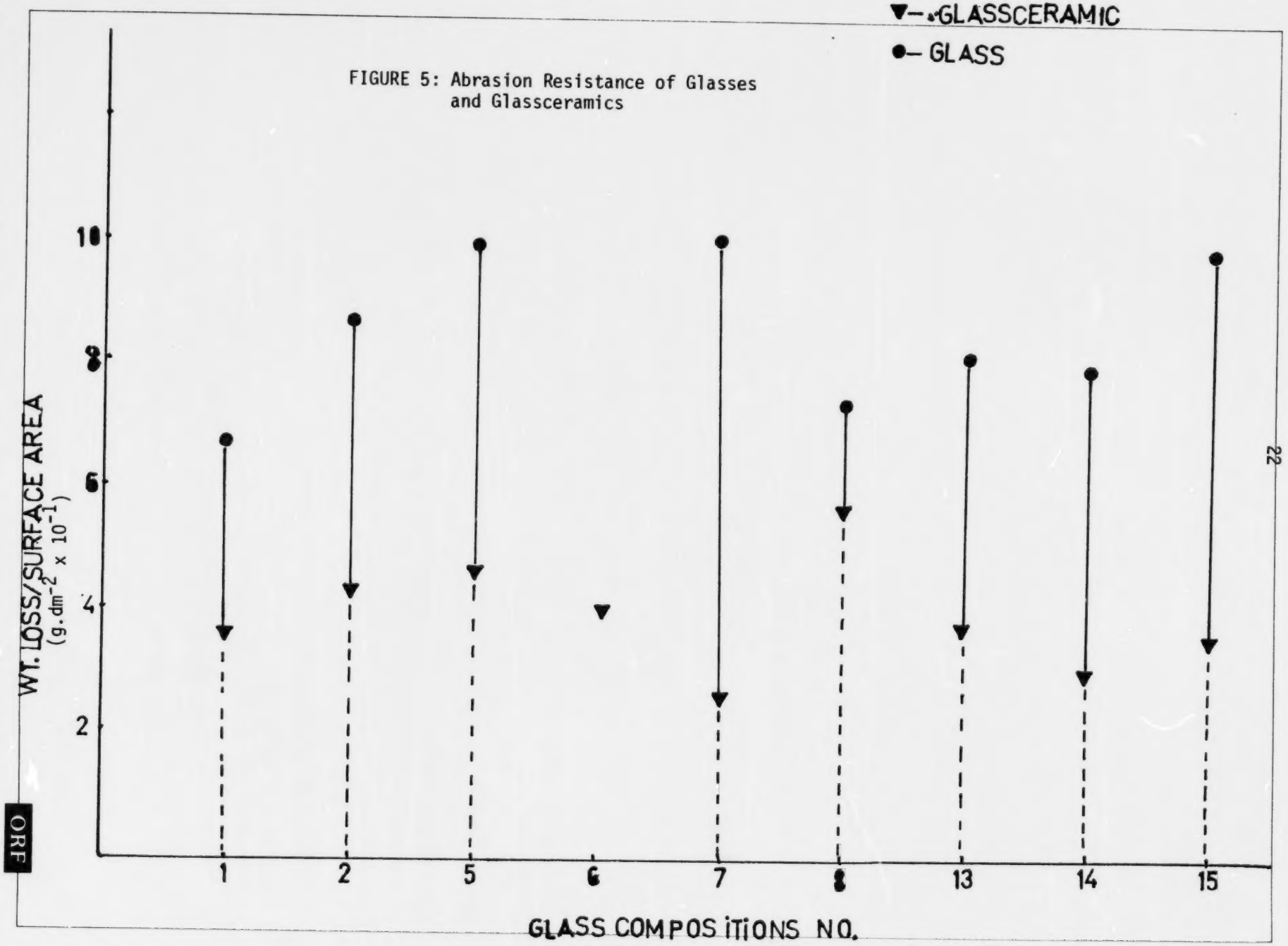

FIGURE 5: Abrasion Resistance of Glasses and Glassceramics

ORE

FIGURE 6: Abrasion Resistance of Glasses vs. Al_2O_3 Concentration.

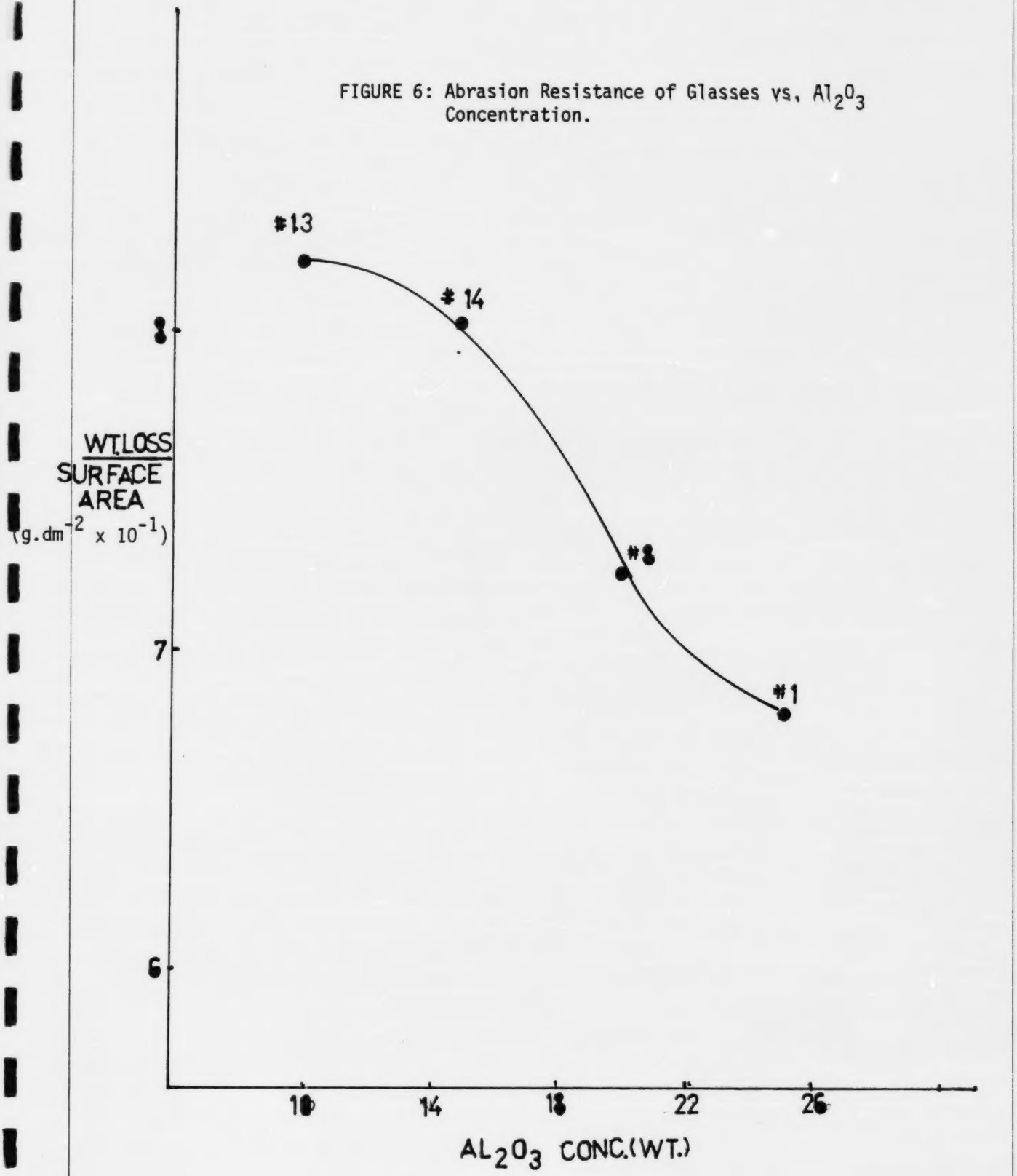

ORF

TABLE 12: Abrasion Resistance of Glass-Ceramics Nos. 8 and 13

Composition	Nucleation		Crystallization		Average Weight Loss/ Surface Area ($g.dm^{-2} \times 10^{-1}$)
	Temperature (^{o}C)	Time (Hrs.)	Temperature (^{o}C)	Time (Hrs.)	
8	800	27	900	65	8.3
	850	4	950	24	5.8
	850	12	950	24	7.1
	850	24	950	24	7.7
	850	24	950	12	5.9
	900	24	950	24	6.5
13	800	27	900	65	4.7
	850	4	950	24	4.2
	850	12	950	24	4.9
	850	24	950	24	5.0
	850	24	950	12	5.3
	900	24	950	24	3.8

ORF

The improvement in abrasion resistance after heat treatment is schematically depicted in Figure 5. The best abrasion resistance for the glasses is found for composition No. 1. This composition has a relatively high concentration of silica and alumina.

The effect of Al_2O_3 concentration of the glasses on the abrasion resistance is graphically illustrated in Figure 6. It can be seen that an increase in the Al_2O_3 concentration is accompanied by an increase in the abrasion resistance.

For the glass-ceramics the abrasion resistance depended not only on composition but also on the heat treatment program. The highest abrasion resistant glass-ceramics are compositions 7 and 14. Table 11 gives a summary of the abrasion resistance of glass-ceramics numbers 8 and 13.

Since only a few compositions have a sufficient number of data points to justify the extrapolation of trends caution should be exercised when interpreting the results. On the basis of the data for compositions numbers 8 and 13 it appears that a reduction in the nucleation time gives an increase in abrasion resistance. Nucleation at 850°C followed by crystallization at 950°C for 24 hours gives the best results for nucleation time of four hours. A variation of the duration of crystallization is less clear. For composition No. 8 an increase in abrasion resistance was observed when the crystallization time was reduced from 24 to 12 hours at 950°C following nucleation at 850°C for 24 hours. A similar reduction in crystallization time for composition 13 showed a slight increase in ~~abrasion resistance~~ weight loss, however.

McMillan has compared the indentation hardness of a number of glass-ceramics with glasses and with a high alumina ceramic (see Table 13). It can be seen that the two glass-ceramics (Corning compositions 9606 and 9608) have a significantly higher indentation hardness than the two glass compositions, although both of them are well below the value of the high alumina ceramic.

One of the glass-ceramic compositions, Corning 9606 is known to be extremely resistant to the abrasive action of sand and erosion due to rain. Its hardness is close to that of tempered instrumental steel (see Appendix A, reference 13).

Although indentation hardness tests and tests for abrasion resistance cannot be fully equated it appears that the trends reported by McMillan can also be observed in this study, i.e. an increase in abrasion resistance when glass-ceramics and the glasses are compared. However, high-density alumina still has the superior abrasion resistance.

TABLE 13: Indentation Hardness of Glasses and Glass-Ceramics

Material	Test load (g)	Hardness Knoop (kg/mm^2)	D.P.H. (kg/mm^2)
Glass-ceramic 9606	100	689	631
	500	619	—
Glass-ceramic 9608	100	703	707
	500	588	639
Glass 7900	100	532	—
(96% silica glass)	500	477	—
Glass 7740	100	481	—
(low expansion borosilicate glass	500	442	—
High alumina ceramics,	100	1880	—
(>93% AL_2O_3)	500	1530	—

5.6 Fracture Testing and Crack Inhibition

Selected samples of glasses and glass-ceramics were fractured on a 4-point bending jig with Instron testing equipment. The modulus of rupture is shown in Table 14.

Glass-ceramic compositions Nos. 2 and 13 were found to have a high modulus of rupture. These glass-ceramics have MOR values that are about 2x as high as those of most glasses which range from 55-70 MNm^{-2} (8,000 - 10,000 psi).

Scanning Electron Microscopy (SEM) was used to investigate the fracture surfaces (see Figures 7-14). Figure 7 shows the fracture surface of glass-ceramic No.2. The fracture initiation and crack propagation can be observed at a high magnification. The fracture surface is mainly transgranular although some intergranular fracture is observed as well.

Phase separation can be detected in Figure 9 (glass-ceramic No. 7). Here, the fracture surface is strongly transgranular as well. Micrographs 11 and 12 show crack inhibition in glass-ceramic No.8. The crack propagated from the initiation site and appeared to be blocked as it transversed the boundaries. The fracture surface is transgranular with steps and cleavages.

Figure 13 showed the rough fracture surface of glass-ceramic No.13. Higher magnification displayed a surface with thin weavings and micropores.

McMillan (reference 1, of Appendix A) has discussed the factors that contribute to fracture toughness of a glass-ceramic. Fracture toughness which is closely related to impact strength will be enhanced if the fracture is compelled to follow a tortuous path through the material. This condition requires inter-crystalline rather than transgranular fracture. Intercrystalline fracture is favoured when randomly oriented crystals with well-defined cleavage planes are present in the glass-ceramic. A second factor is the relative magnitude of the

TABLE 14: Results of 4-Point Bending Tests

Composition*	Nucleation		Crystallization		Modulus of Rupture	
	Temperature (°C)	Time (hrs.)	Temperature (°C)	Time (hrs.)	$MN.m^{-2}$	(psi)
2 gc	900	24	950	24	114	16,500
5 gc	750	24	800	24	54	7,900
7 gc	850	24	950	24	94	13,600
8 gc	900	24	950	24	94	13,600
10 g	-	-	-	-	51	7,400
11 g	-	-	-	-	85	12,400
13 gc	850	24	950	24	120	17,400

*g : glass
gc : glass-ceramic

coefficient of thermal expansion of the crystalline and glassy phases. If the crystal phase has the higher thermal expansion coefficient then the radi al stresses in both phases are compressive. The circumferential stresses are compressive in the glass and tensile in the crystal. Such a situation favours intergranular fracture.

Several of the crystalline phases detected in the glass-ceramics of this study (see Table 9), such as diopside, anorthite, wollastonite, etc. exhibit good to nearly perfect cleavage in at least one crystallographic direction. Thus, intergranular fracture would be favoured on the basis of those characteristics. The picture for the thermal expansion coefficients is less clear. Values of 45×10^{-7}, 94×10^{-7}, and -19×10^{-7} cm/cm/^{o}C for anorthite, wollastonite and pseudoanatase, respectively, suggest that there is quite a bit of variation amoung the C.T.E. values of the crystalline phases in the glass. A comparison of C.T.E. values between the glass-ceramics and the parent glasses show an increase for some compositions (numbers 1,5,6,7,14,15) while a decrease is observed for others (numbers 2,8,13) (see Tables 5 and 14). It can be argued that an increase in the C.T.E. of a glass-ceramic when compared with the parent glass reflects an increase in the weighted average of the C.T.E. values for the individual crystalline phases. More than one phase were usually detected in the glass-ceramics and there is a great deal of variations in the C.T.E. values. Also for most compositions the C.T.E. values of the glass-ceramic and parent glass do not differ greatly. These facts, together with the observation of predominantly transgranular fracture seems to indicate that the fracture toughness of the compositions developed here is not optimal from a microstructural perspective.

ORF

FIGURE 7: Electron Micrograph of Fracture Surface of Glass-ceramic No.2

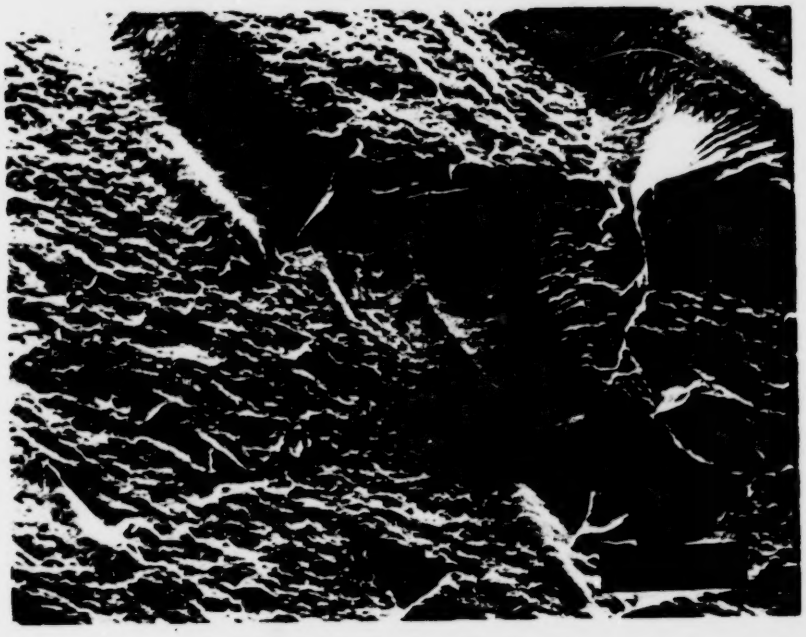

FIGURE 8: Electron Micrograph of Fracture Surface of Glass-ceramic No.2, Higher Magnification.

FIGURE 9: Electron Micrograph of Fracture Surface of Glass-ceramic No. 7

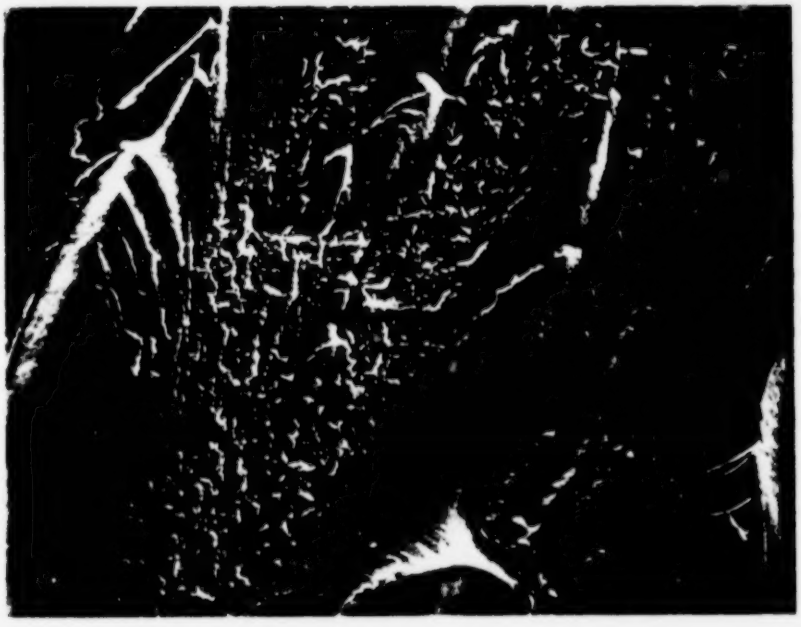

FIGURE 10: Electron Micrograph of Fracture Surface of Glass-ceramic No. 7, Higher Magnification.

FIGURE 11: Electron Micrograph of Fracture Surface of Glass-ceramic, No. 8

FIGURE 12: Electron Micrograph of Fracture Surface of Glass-ceramic No. 8, Higher Magnification.

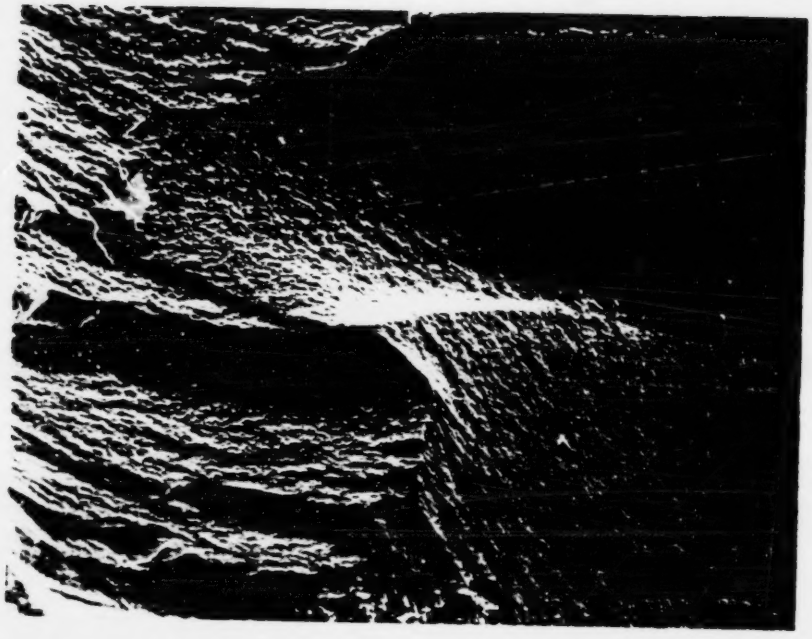

FIGURE 13: Electron Micrograph of Fracture Surface of Glass-ceramic No. 13

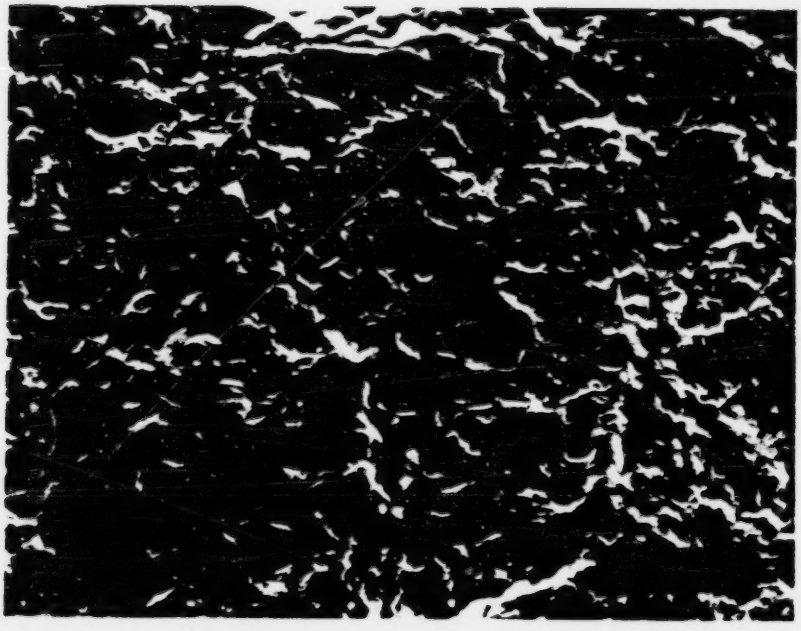

FIGURE 14: Electron Micrograph of Fracture Surface of Glass-ceramic No. 13, Higher Magnification.

6. CONCLUSIONS AND RECOMMENDATIONS

Glass-ceramics with good abrasion resistance have been produced and evaluated. It was found that the heat treatment cycle, especially the nucleation time affected the abrasion resistance of the glass-ceramics. The experimental results indicated that glass-ceramics based on basalt and slag possess high mechanical strength. These features are attractive because basalt and slag are inexpensive and readily available materials. Composition No.15 of this study was produced from blast-furnace slag from a Hamilton Steel Plant. Since slag is a large unutilized waste product of several metallurgical operations it appears that there is potential for an industrial process in Ontario for the production of abrasion resistant glass-ceramics from this source.

The products from this process can be used for pipes and tubes intended for the passage of abrasive slurries and drosses. However, further research and development will be necessary to develop and optimize economically viable glass-ceramic compositions.

7. ACKNOWLEDGEMENTS

The authors would like to acknowledge the assistance of Mrs. S. Hemraj and Mr. R. Hopton in preparing and testing of the samples.

D. Nguyen
Assistant Research Scientist

J.H.G. van Roode,
Research Scientist

Glass & Ceramics Division
Department of Metals, Glass & Ceramics

/dc

APPENDIX A

ABRASION RESISTANT GLASS-CERAMICS

LITERATURE REVIEW

TABLE OF CONTENTS

		Page
1.	INTRODUCTION	2A
2.	THEORETICAL ASPECTS OF GLASS-CERAMICS	3A
	2.1 Selection of Glass Compositions	3A
	2.2 Heat Treatment Process	5A
	2.3 Methods of Studying the Heat Treatment Process	8A
	2.4 Applications of Glass-Ceramics	11A
3.	ALUMINO-SILICATE GLASS-CERAMICS	12A
	3.1 Compositions	12A
	3.2 Physical Properties	15A
4.	BASALTIC GLASS-CERAMICS	17A
	4.1 Compositions	17A
	4.2 Heat Treatment and Physical Properties	18A
5.	SLAG GLASS-CERAMICS	20A
	5.1 Compositions	20A
	5.2 Heat Treatment and Physical Properties	24A
6.	ABRASION AND WEAR RESISTANCE OF GLASS-CERAMICS AND CERAMICS	25A
	6.1 Wear Resistance	25A
	6.2 Abrasion Resistance	27A
	6.3 Methods of Measurement	28A
7.	FRACTURE AND CRACK INHIBITION OF GLASS-CERAMICS	28A
	7.1 Fracture of Glasses	28A
	7.2 Strength and Fracture Properties of Glass-ceramics	29A
	7.3 Method of Testing the Strength of Glass	32A
	7.4 Fracture Topography Techniques	34A
	7.5 Crack Inhibition in Glass-ceramics	35A
8.	REFERENCES	40A

ORF

1. INTRODUCTION

Glass-ceramics, also known as "devitrified glass" or crystalline glass" (U.S.A.), Sitalls (U.S.S.R.), and "vitroceramics" or devitroceramics" (Europe) is the name for a class of materials which can be produced from a glass through a process of controlled heat treatment. From an industrial point of view glass-ceramics have several advantages over crystalline ceramics. Their properties are constant and well-defined for a particular composition subjected to a prescribed heat treatment process which is important for large scale production. The products are non-porous and their crystal size can be controlled. The dimensional changes occurring during the transformation of the glass to the glass-ceramic are small compared to the shrinkage observed for most conventional ceramics during drying and firing stages.

In general, glass-ceramics have a higher mechanical strength and a greater abrasion resistance than the parent glasses. Also their thermal expansion coefficient can be varied over a much wider range than for glasses.

In this survey glass-ceramic compositions based on the alumino-silicate, basalt and slag systems will be reviewed. The abrasion resistance and fracture properties of these materials will also be discussed.

2. THEORETICAL ASPECTS OF GLASS-CERAMICS

2.1 Selection of Glass Compositions[1]

The development of glass-ceramics has advanced greatly through an increased understanding of the relationship between glass composition, melting temperature, chemical stability, and the heat treatment process. The latter factor is of great importance for the nucleation and crystallization of glasses.

Melting Temperatures:

The range of melting temperatures of interest is usually between 1400 and 1600°C. The addition of fluxes, such as Li_2O, Na_2O, K_2O, ZnO, PbO, and B_2O_3 will lower the melting temperature of a glass. The addition of these fluxes will also lower the viscosity at a certain temperature which is important if speed of melting and refining are considered. The addition of Al_2O_3 has the opposite effect. It will increase the viscosity.

Chemical Stability:

Although the addition of fluxes imparts desirable properties on a glass, high proportions of Na_2O or K_2O should be avoided in view of their adverse effects on chemical stability.

Nucleation and Crystallization:

The choice of an appropriate nucleating agent is important for the preparation of glass-ceramics. Most commonly, the nucleating agent is not present in the batch composition (heterogeneous nucleation).

A nucleating agent for glass-ceramic preparation should have the following properties[2].

- The nucleating agent should be readily soluble in the glass at high temperatures and insoluble at low temperatures.

- The interfacial tension between the foreign particles (nucleating agent) and the phases to be nucleated must be low. In other words, the phases to be nucleated must wet the foreign particles so that atoms of the new crystals can readily attach themselves to the surface of the nucleating agents.

- The crystal structure and inter-atomic distance of the foreign particles and the phases to be nucleated must be similar.

The other criterion for the selection of a glass composition is that it can be readily crystallized. In general, readily crystallizable glasses contain a relatively high proportion of modifying oxides.

ORF

2.2 The Heat Treatment Process

The object of the heat treatment is to convert the glass into a micro-crystalline glass-ceramic having properties superior to those of the original glass.

Tamman's [3] studies of the crystallization of supercoated liquids contributed greatly to the knowledge of nucleation and crystallization processes. He determined a zone below the equilibrium temperature referred to as the metastable zone in which nuclei do not form at a detectable rate. At the temperature below this zone the crystallization is controlled by several factors:

- the number of nuclei formed
- the rate of crystal growth
- the viscosity of the glass.

Since the objective in glass-ceramic preparation is to produce a large number of small crystals it is advantageous to nucleate the glass at the optimum nucleation temperature (see Figure 1). On the other hand, to obtain a glass-ceramic with maximum strength the glass must be cooled below the maximum nucleation temperature before starting the nucleation heating phase. The heating rate which is not critical at this point depends on the thickness of the glass and its thermal expansion coefficient. Glass with low thermal expansion can withstand more rapid temperature increases.

As the temperature range for crystallization is above the range for nucleation, the temperature should be increased to permit crystal growth upon the nuclei in the crystallization phase. A schematic for the nucleation-crystallization process is given in Figure 2.

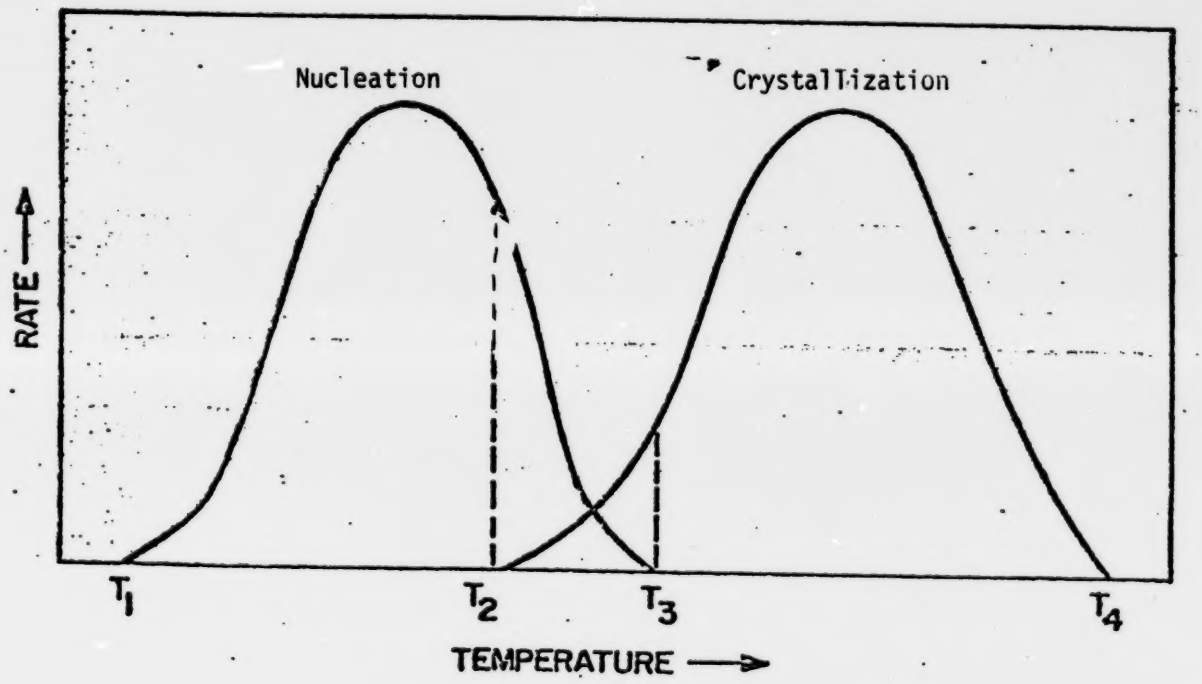

FIGURE 1: Nucleation and Crystallization Rate Curves.

T_1 and T_3 : Minimum and maximum nucleation temperatures

T_2 and T_4 : Minimum and maximum crystallization temperatures

ORF

(a) Crystallization Stage
(b) Nucleation Stage

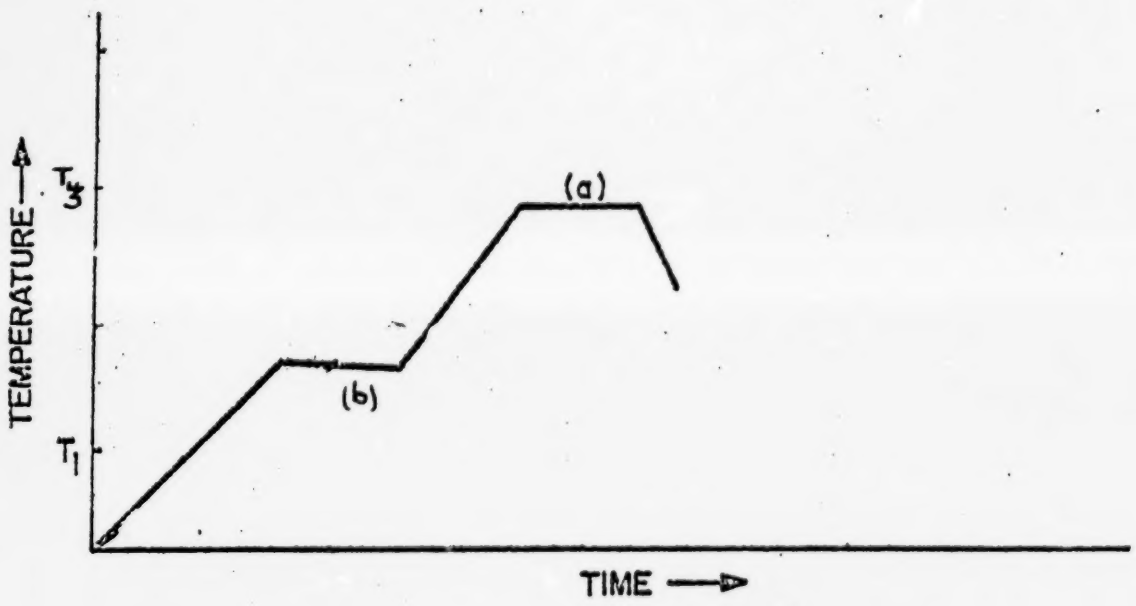

FIGURE 2: Heat Treatment Cycles for Controlled Crystallization.

ORF

To avoid deformation of the glass-ceamic the rate of temperature increase must be carefully controlled. If the rate of heating is too high, the rate of crystal growth may not be sufficiently rapid and defects, such as deformation and cracking will occur. Cracking is a result of stresses that arise because of differences in density between the crystal and the glass phases. With slow heating these stresses are relieved through viscous flow of the glass phase. However, too low a heating may result in a large amount of glass remaining after heat treatment.

The glass-ceramic can be cooled rapidly to room temperature upon completion of the process.

2.3 Methods for Studying the Heat Treatment Process[1]

The heat treatment process is the critical stage in the production of glass-ceramics and must be carefully controlled to ensure that the desired types and proportions of crystals are formed. Several techniques are used to investigate the devitrification of glass. X-ray diffraction analysis, optical and electron microscopy, hot stage microscopy, Differential Thermal Analysis (DTA) and laser light scattering.

X-ray Diffraction Analysis:

X-ray technique can be applied to study the heat treatment behaviour of the glass-ceramic. This technique can be used for:

- Determination of the onset of crystallization.
- Identification of the crystalline species present.
- Estimation of the percentage of crystallinity.
- Structural determination of the crystalline species.

Typical X-ray patterns of a glass and a glass-ceramic are shown in Figure 3. The X-ray pattern of the glass is characterized by a complete absence of sharp lines.

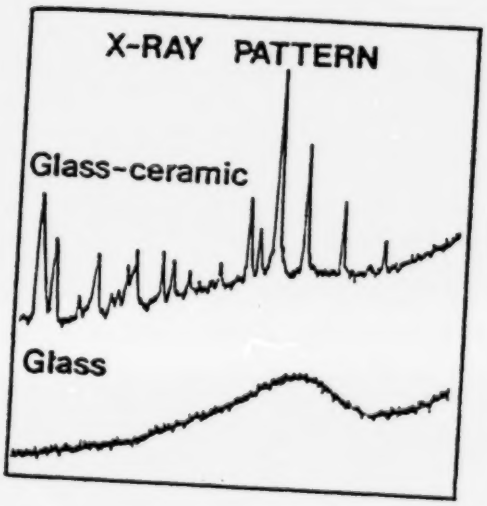

FIGURE 3: X-ray Patterns of a Glass and a Glass-ceramic

Optical and Electron Microscopy:

For most glass-ceramics the structural features of interest are often below the limit of resolution of the optical microscope.

More useful for glass-ceramic microstructural studies is electron microscopy. Scanning Electron Microscopy (SEM) is of great value. Many important structural features of a glass-ceramic can be elucidated using this technique. For the investigation of phase separation or nucleation processes, the higher resolution of the Transmission Electron Microscope (TEM) is utilized. Identification of individual crystals by electron

diffraction analysis or by Energy Dispersive Analysis of X-rays (EDAX)are other techniques that can be applied in conjunction with electron microscopy to study the heat treatment process of glass-ceramics.

Differential Thermal Analysis DTA):

The use of DTA to study the crystal growth kinetics of glasses have been reported by several workers[1,4,5,6]. The crystallization of a substance is accompanied by an exothermic effect since the free energy of the regular crystal lattice is less than that of the disordered liquid state (Figure 4). Conversely, the melting of the crystals gives rise to an endothermic effect. With DTA, phase transformations and chemical reactions that occur with an increase in temperature can be monitored.

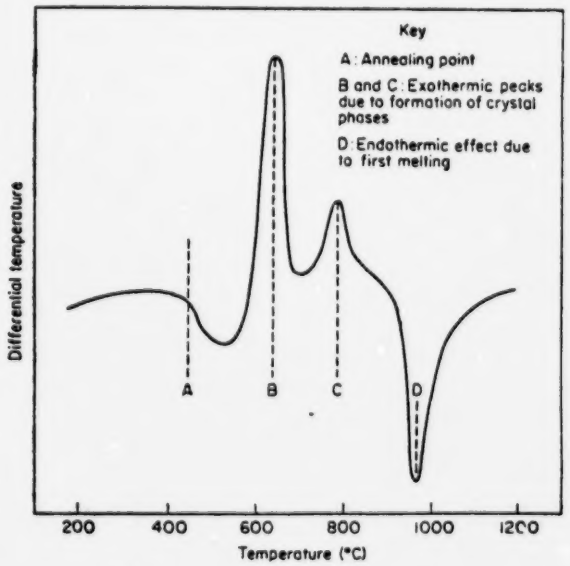

(1)
FIGURE 4: Differential Thermal Analysis Curve for a devitrifiable Glass.

ORF

Light Scattering:

If a beam of light enters a medium with a liquid-type structure, such as a glass, scattering of light will occur in directions away from that of the incident beam due to point-to-point variation in the refractive index of the medium.

A simple experiment, in which, the intensity of scattered light is measured in a direction of $90^{o}C$ to the incident beam can be used to detect the presence of scattering particles. This method can be used to measure the crystallization rate and the average crystal size.

Hot Stage Microscopy:

To study the development of the glass-ceramic microstructures directly it is possible to use an optical microscope provided with a hot stage. The set-up can be simple, a small electrically heated thermocouple bent into a loop to hold the specimen. This technique has been used by several investigators.

2.4 Applications of Glass-ceramics

Glass-ceramics have a variety of technical and industrial applications. One of the earliest successful applications of glass-ceramics was in the manufacture of cooking ware with high thermal shock and good abrasion resistance [2]. Another important area in which glass-ceramics have been applied is in the fabrication of heat exchangers[8,9].

ORF

The superior electrical properties of some glass-ceramics have led to their use in electrical applications. Strong, abrasion resistant basaltic glass-ceramics materials have also been used for the fabrication of tiles for lining process equipment, such as cyclone separators[11], and for internal protection of pipes[12].

3. ALUMINO-SILICATE GLASS-CERAMICS[1,13]

At the present time, glassceramics are prepared from glasses of more than 5,000 different compositions. Some glassceramic compositions are given in Table 1.

Alumino-silicate glassceramics, one of the most popular family of compositions, can be divided into several categories.

3.1 Compositions

Li_2O-Al_2O-SiO_2 and MgO-Al_2O_3-SiO_2

Glass-ceramics in these systems are characterized by a low thermal expansion coefficient.

In addition to the major constituents, the glass compositions include a nucleation catalyst which may be a metal, titanium oxide or a metallic phosphate. The minor constituents may also contain alkali earth oxides and alkali metal oxides. The constituents modify the melting range, the working properties and the crystallization characteristics of the derived glass-ceramics. Several of the glass-ceramic compositions in this system are listed in Table 1 (composition a1 and d6).

$RO-Al_2O_3-SiO_2$

Where RO is CaO, ZnO, CdO, BaO, PbO, MnO, FeO, CaO with TiO_2 or ZrO_2 as the additives. The glass-ceramics have high mechanical strength, high hardness and good wear resistance. Several compositions are given in Table 1 (compositions e1 to f8).

TABLE 1:[1] Examples of Glass-ceramic Compositions.

Glass reference	SiO_2	Al_2O_3	MgO	CaO	BaO	ZnO	PbO	CdO	Li_2O	K_2O	B_2O_3	TiO_2	P_2O_5	ZrO_2	F	Literature reference
a1	73·5	16·2	—	—	—	—	—	—	4·3	—	—	6·0	—	—	—	1
a2	67·8	20·8	—	—	1·0	1·0	—	—	3·9	—	—	5·5	—	—	—	1
a3	68·0	21·0	—	—	—	—	—	—	4·0	1·0	—	6·0	—	—	—	1
a4	63·6	19·8	2·8	2·7	—	—	—	—	8·1	—	—	—	3·0	—	—	3
a5	55·9	18·9	—	—	—	—	—	—	22·2	—	—	—	3·0	—	—	3
b1	42·8	30·2	14·0	—	—	—	—	—	—	—	—	13·0	—	—	—	2
b2	45·2	29·5	10·4	—	—	—	—	—	—	1·8	—	10·8	—	—	2·3	2
b3	46·7	28·9	13·3	—	—	—	—	—	0·9	—	—	10·2	—	—	—	2
b4	64·8	18·5	9·3	—	—	—	—	—	—	—	—	7·4	—	—	—	2
b5	52·3	20·3	24·4	—	—	—	—	—	—	—	—	—	3·0	—	—	3
b6	59·4	17·9	19·7	—	—	—	—	—	—	—	—	—	3·0	—	—	3
c1	73·1	—	7·0	—	—	—	—	—	10·5	—	6·4	—	3·0	—	—	3
c2	67·9	—	15·5	—	—	—	—	—	13·6	—	—	—	3·0	—	—	3
c3	64·7	7·7	11·7	—	—	—	—	—	12·9	—	—	—	3·0	—	—	3
d1	58·1	—	—	—	—	15·8	—	—	23·1	—	—	—	3·0	—	—	3
d2	48·2	—	—	—	—	39·2	—	—	9·6	—	—	—	3·0	—	—	4
d3	44·4	—	—	—	—	48·1	—	—	4·5	—	—	—	3·0	—	—	4
d4	37·2	—	—	—	—	50·5	—	—	9·3	—	—	—	3·0	—	—	4
d5	59·2	—	—	—	—	13·1	14·0	—	9·0	2·0	—	—	2·7	—	—	5
d6	47·8	—	—	—	—	11·0	29·9	—	7·3	1·6	—	—	2·4	—	—	6
e1	50·9	23·2	—	—	—	18·5	—	—	—	—	—	7·4	—	—	—	2
e2	49·0	19·6	—	—	—	29·4	—	—	—	—	—	2·0	—	—	—	2
e3	27·0	17·0	—	—	—	36·0	—	—	—	—	16·0	—	—	4·0	—	7
e4	—	6·0	—	—	—	50·0	—	—	—	—	40·0	—	—	4·0	—	7
e5	—	6·0	—	5·0	—	50·0	—	—	—	—	39·0	—	—	—	—	7
f1	53·4	17·7	—	17·8	—	—	—	—	—	—	—	11·1	—	—	—	2
f2	66·7	15·5	—	6·7	—	—	—	—	—	—	—	11·1	—	—	—	2
f3	48·2	17·6	—	—	21·9	—	—	—	—	—	—	12·3	—	—	—	2
f4	39·5	21·9	—	—	26·3	—	—	—	—	—	—	12·3	—	—	—	2
f5	31·1	15·5	—	—	—	—	42·3	—	—	—	—	11·1	—	—	—	2
f6	15·6	4·4	—	—	—	—	68·9	—	—	—	—	11·1	—	—	—	2
f7	27·3	27·3	—	—	—	—	—	36·3	—	—	—	9·1	—	—	—	2
f8	44·7	22·3	—	—	—	—	—	22·3	—	—	—	10·7	—	—	—	2

References: 1. Stookey (1959b), 2. Stookey (1960), 3. McMillan and Partridge (1963a), 4. McMillan and Partridge (1963b), 5. McMillan and Hodgson (1966), 6. McMillan and Hodgson (1967), 7. McMillan and Partridge (1969).

ORF

Table 2 depicts the variety of crystal phases in the glass-ceramics. Since each type of glass-ceramic contains different crystal phases, materials having a wide range of physical properties can be produced.

TABLE 2:[1] Crystal Phases which occur in Alumino-Silicate Glass-ceramics.

Glass-ceramic type	Crystal phases
$CaO–Al_2O_3–SiO_2–TiO_2$	Anorthite, $CaO\ Al_2O_3\ 2\ SiO_2$ Cristobalite, SiO_2 Sphene, $CaO\ TiO_2\ SiO_2$ Tridymite, SiO_2
$ZnO–Al_2O_3–SiO_2–TiO_2$	Gahnite, $ZnO\ Al_2O_3$ Willemite, $2\ ZnO\ SiO_2$ Cristobalite, SiO_2
$BaO–Al_2O_3–SiO_2–TiO_2$	Dibarium trisilicate, $2\ BaO\ 3\ SiO_2$
$PbO–Al_2O_3–SiO_2–TiO_2$	Lead titanate, $PbOTiO_2$
$MnO–Al_2O_3–SiO_2–TiO_2$	Pyrophanite, $MnO\ TiO_2$ Cristobalite, SiO_2 Manganese cordierite, $2\ MnO\ 2\ Al_2O_3\ 5\ SiO_2$ Mullite, $3\ Al_2O_3\ 2\ SiO_2$ Tridymite, SiO_2 Quartz, SiO_2

Al_2O_3-SiO_2

This binary glass-ceramic system was studied by MacDowell and Beall[14]. The composition has an Al_2O_3 content ranging from 5 to 60 mole percent and was heat treated at temperatures between 900°C and 1600°C.

ORF

3.2 Physical Properties

The properties of several glass-ceramic compositions manufactured by Corning are shown in Table 3[(2)]. They have a modulus of rupture range from 11 to 6 x 10^{-8} dyne/cm^2. The Linear thermal expansion coefficient is from 4 to 104 x $10^{-7}/^{o}C$. Table 4 is a summary of Alumino silicate glass-ceramic composition and their crystalline phases.

TABLE 3: Physical Properties of Some Glass-ceramics.

PROPERTY	PYROCERAM* 9606	PYROCERAM* 9608	FOTOCERAM* 8603
Specific gravity at 25° C.	*2.61*	*2.50*	*2.45*
Water absorption, %	*0.00*	*0.00*	*0.00*
Porosity (gas permeability)	*gastight*	*gastight*	*gastight*
Softening temperature, ° C.	*1250*	*1250*	*900*
Specific heat at 25° C.	*0.185*	*0.190*	—
Mean value, between 25 ° and 400° C.	*0.230*	*0.235*	—
Thermal conductivity, cal./(cm. sec.° C.) at 25° C.	*0.0087*	*0.0047*	—
Linear coefficient of thermal expansion × 10^{-7}/° C., between 25° and 300° C.	*57*	*4-20***	*104*
Modulus of elasticity, dynes/cm.² × 10^{-11}	*11.9*	*8.6*	*6.9*
Poisson's ratio	*0.245*	*0.25*	*0.22*
Modulus of rupture (abraded), dynes/cm.² × 10^{-8}	*13*	*11-16*	*13*
Hardness			
Knoop 100 g.	*698*	*703*	—
500 g.	*619*	*588*	—
Dielectric constant			
Frequency 10^{6} c.p.s. at 25° C.	*5.58*	*6.78*	*5.6*
300° C.	*5.60*	—	*6.6*
500° C.	*8.80*	—	—
Frequency 10^{10} c.p.s. at 25° C.	*5.45*	*6.54*	*5.6*
300° C.	*5.51*	*6.65*	*5.8*
500° C.	*5.53*	*6.78*	*6.4*
Loss factor			
Frequency 10^{6} c.p.s. at 25° C.	*0.008*	*0.02*	*0.029*
300° C.	*0.086*	—	*0.40*
500° C.	—	—	—
Frequency 10^{10} c.p.s. at 25° C.	*0.002*	*0.045*	*0.045*
300° C.	*0.004*	*0.077*	*0.10*
500° C.	*0.008*	*0.27*	*0.23*
Volume resistivity, Log_{10} (ohm-cm.) at 250° C.	*10*	*8.1*	—
350° C.	*8.6*	*6.8*	—

*Corning Glass Works, N.Y.

ORF

TABLE 4: Alumino Silicate Glass-ceramic[1,2,10]

Major Constituents	SiO_2-Al_2O_3-RO (RO is CaO, ZnO, CdO, BaO, PbO, MnO-FeO, CaO, Li_2O, MgO)
Concentration Wt.%	(40-75) - (4-36) - (0 to 68.9) SiO_2 Al_2O_3 RO
Nucleating Agents (Wt.%)	TiO_2, P_2O_5, ZrO_2 (2-15) (0.5-6) (4)
Heat Treatment (Depending on glass composition)	Melting 1250-1600°C Nucleation ~800°C (50°C above annealing temp.) Crystallization ~1200°C Heating rate 2°C - 5°C/min.
Crystalline Phases	Anorthite ($CaO.Al_2O_3.2SiO_2$), Critobalite (SiO_2) Sphene ($CaO.TiO_2.SiO_2$), Tridymite (SiO_2) Willemite ($2ZnO.SiO_2$), Lead Titanate ($PbTiO_3$), Manganese Cordierite ($2MnO.2Al_2O_3.5SiO_2$), Mullite ($3Al_2O_3.2SiO_2$), Quartz (SiO_2).
Physical Properties	Hardness: Knoop 588 - 703[2] DPH (Kg/mm²).631-707) Scratch Moh's 7.5 Modulus of Rupture: 11-16 x 10^{-8} (dym/cm²)[2] Thermal Expansion: 6-57 x 10^{-7} /°C (25-300°C) Softening Point: 1250°C

ORF

4. BASALTIC GLASS-CERAMICS

Basalt is a grey to black, fine-grained volcanic rock which is the major constituent of oceanic islands. Basaltic rocks can be easily melted and formed into stable glasses. These glasses can be reheated to form fine-grained, black glass-ceramics with good chemical durability, high mechanical strength, and excellent abrasion resistance.

4.1 Compositions

The compositions of the basaltic rocks from different parts of the world are shown in Table 5.

TABLE 5:[15] Compositions of Basaltic Rocks

Composition	Results					
	Tholeiite			Olivine Basalt	Alkali basalt	
Oxide (Wt.%)	Westfield, Mass.*	Karroo Trap, S. Africa	Deccan Plateau, India	Kilauca, Hawaii	St. Helena Island	Uganda, E. Africa
SiO_2	51.6	52.25	50.67	49.83	47.62	44.75
Al_2O_3	14.1	14.60	13.30	12.92	16.27	11.74
TiO_2	1.0	1.10	2.52	2.85	3.57	2.58
Fe_2O_3	4.4	0.84	3.52	3.14	3.87	2.06
FeO	8.4	9.89	10.34	8.34	8.17	8.95
MnO	0.2	0.45	0.19	0.18	0.11	0.16
MgO	6.4	6.95	6.00	9.24	6.33	13.32
CaO	9.3	9.71	10.15	11.02	8.65	10.24
Na_2O	3.2	2.21	2.40	2.22	3.82	2.54
K_2O	1.2	0.96	0.60	0.52	1.14	2.92
B_2O_5	0.2	0.22	0.31	0.26	0.45	0.62

*Analyzed at Corning Glass Works, Corning, N.Y.

The major constituents of the basaltic glass-ceramics are SiO_2, Al_2O_3, MgO, CaO and Iron Oxides (Fe_2O_3 and FeO).

The basaltic glass-ceramic compositions are summarized in Table 6. The nucleating agent normally used is titanium dioxide (TiO_2). The major crystalline phases are Clinopyroxene and Magnetite.

4.2 Heat Treatment and Physical Properties

The preferred nucleation temperature range is from 650 to 700°C[10] and the crystallization temperature is from 700 to 1000°C. The basaltic glass is heated in the atmosphere at 5°C/min. to a temperature between 640-675°C and is maintained at this temperature for a sufficient length of time normally about ½-4hours to secure good nucleation.

Following nucleation, the glass is heated at a rate of 5°C/min. to a temperature between ∿850 and ∿1050°C and is maintained at that level for ½ to 2 hours to ensure maximum crystallization.

For example, Omar, et.al.[16] found that for Abu-Zarbal balsaltic rock, the optimum heat treatment comprises of the gradual heating of the annealed glass up to 900°C, a soak at this temperature for a further two hours. The temperature is then increased up to 1050°C for three hours and is cooled at a relatively high speed.

The most striking features of the basaltic glass-ceramics are their excellent abrasion and chemical resistance. Their hardness on Moh's scale is about 8.5. The Diamond Pyramid Hardness (DPH) under load of 1 kg. can be as high as 82.2.

ORF

TABLE 6: Basaltic Glass-ceramics[15,17]

Major Constituents & (Concentration Wt.%)	SiO_2 (46-53.5) - Al_2O_3 (9.95-16.27) - MgO (5.2-12.13) CaO (8.65-18.30) - Iron Oxides as Fe_2O_3 & FeO (7.97-73.8)
Nucleating Agent	TiO_2 (0.9-3.57)
Heat Treatment & Time	Melting 1350-1600[12] (½-6 hrs.) Nucleation & Crystallization: 640-675[12] (½-4 hrs) and 850-1000[12] (½-2 hrs) Up to 900°C[14] (2 hours) and 1050°C[14] (3 hours)
Crystalline Phase	Clinopyroxene, Magnetite
Physical Properties	Hardness Knoop: 900[12] DPH (1 kg.) : 822 Modulus of Rupture (Abraded glass): 14,000-19,000 psi Moh's scale : 8.5 Softening Temperature : 1000°C[12]

5. SLAG GLASS-CERAMICS

5.1 Compositions

Glass-ceramics from blast-furnace slags are essentially devitrified products from the system $CaO-MgO-Al_2O_3-SiO_2$ to which suitable nucleating agents, such as TiO_2, Cr_2O_3, Fe_2O_3, CaF_2, P_2O_5 or ZrO_2 have been added. TiO_2, chrome ore, and CaF_2 are the most efficient nucleating agents. Figure 5 shows the phase diagram for the system $CaO-Al_2O_3$ - SiO_2 (with 5% of MgO).

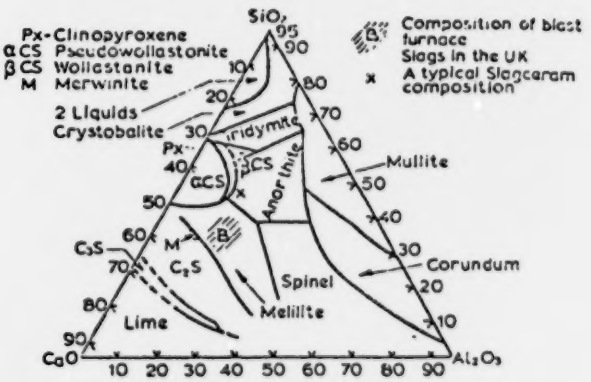

FIGURE 5: The section MgO=5% of the liquidus diagram for the system $Cao-Al_2O_3-MgO-SiO_2$. (Reference 17).

The major constituents of slag glass-ceramics are[18]:

SiO_2	:	45 - 55 wt.%
CaO	:	15 - 45 wt.%
Al_2O_3	:	5 - 30 wt.%
MgO	:	- 10 wt.% (Preferably 5 wt.%)

Slag-ceramics produced in the U.S.S.R. have been compounded from the following amounts of batch materials [19]:

blast-furnace slag	: 50 - 70 wt.%
sand	: 20 - 40 wt.%
nucleating agent	: 0 - 2 wt.%

The composition of batch materials for slag glass-ceramics developed in England is[17]:

Slag	: 100 parts (by weight)
Sand	: 30 parts (by weight)
TiO_2	: 6 parts (by weight)
Chrome Ore	: 0.5 parts (by weight)

Table 7 is a compilation of nucleating agents which have been used successfully for the production of slag glass-ceramics.

In Hungary,[18] a glass-ceramic based on the system $CaO-MgO-Al_2O_3-SiO_2$ has been produced using a heavy metal sulfide as a nucleating agent. Excellent abrasion and chemical resistance are the most valuable features of this material. Crystal size has a considerable influence on these properties of the glass-ceramic. The Hungarian compositions (Minelbite 1 and 2) are shown in Table 8.

ORF

TABLE 7: Nucleating Agents for Slag Glass-ceramics

COUNTRY	NUCLEATING AGENT
U.S.S.R.[16,17]	Oxides of Zinc, Iron, Manganese, Chromium
England[17]	Iron Oxides, iron ores, chrome ores, chrome oxide, titania, clacium fluoride, a combination of 6% titania and 0.5% chrome ore is the most effective.
Hungary[20]	Iron and Manganese Sulphides, ZrO_2, P_2O_5, NiO, V_2O_5, chromite, magnetic.

TABLE 8: Slag Glass-ceramics Developed in Hungary[20]
(composition in wt.%)

OXIDES	MINELBITE 1	MINELBITE 2
SiO_2	56.1	60.9
Al_2O_3	7.9	14.2
CaO	21.9	9.0
MgO	2.6	5.7
BaO	1.5	0.4
MnO	2.0	2.0
Na_2O	5.0	3.2
K_2O	1.0	1.9
Fe_2O_3	1.5	2.5
TiO_2	0.5	0.2

Minelbite 1 has excellent acid resistance while Minelbite 2 is remarkable for its particular high abrasion resistance. The experimental glass-ceramics were made from the following raw materials (in parts by weight):

Blast-furnace slag	:	100 parts
Sand	:	50 parts
Sodium Carbonate	:	8.5 parts
Sodium Sulphate	:	10 parts
Clay	:	10 parts

Chemical composition of blast-furnace (in wt.%):

SiO_2	:	34.0
Al_2O_3	:	9.9
TiO_2	:	1.0
CaO	:	40.6
MgO	:	3.9
BaO	:	2.3
MnO	:	3.6
Fe_2O_3	:	2.2
Na_2O	:	0.3
K_2O	:	0.3
S	:	1.9

The approximate chemical composition of the clay is (in wt.%):

SiO_2	:	80
Al_2O_3	:	20

ORF

5.2 Heat Treatment and Physical Properties

Different heat treatment schedules are recommended depending on the glass composition and nucleating agent. For example, Veasy[21] recommended a nucleation treatment of 10 hours at 720°C for a slag-based glass-ceramic doped with chrome ore and titania. The crystallization phase was initiated by a slow rise in temperature (1°C/min.) to 920°C and a holding stage of 2 to 3 hours. Controlled cooling was necessary to prevent cracking of the finished product.

Mascol, et.al.[23] described the process of nucleation and crystallization in slag glass-ceramics containing Fe and S or Fe and Cr. The following stages can be discussed:

(a) Formation of Fe-FeS droplets
(b) Heterogeneous nucleation of silicate
(c) Growth of silicate crystals.

In contrast, in glass containing iron oxide and chromium oxide as nucleating agents, no phase separation could be observed prior to the appearance of silicate crystals.

The slag glass-ceramics have good strength characteristics, a high degree of hardness, a high degree of resistance to chemical attack and oxidation, and a high resistance to wear and corrosion[18].

The slag glass-ceramic compositions and their physical properties have been summarized in Table 9.

The production of slag glass-ceramics from the lead, zinc and iron containing slags for construction materials has been attempted[22]. The devitrification characteristics of these slags appeared promising but additional work is required to produce bodies with high strength and high density.

6. ABRASION AND WEAR RESISTANCE OF GLASS-CERAMICS AND CERAMICS

Only a small number of studies have been published on wear and abrasion resistance of glass-ceramics since only recently their potential as abrasion resistant components for structural materials has been realized.

6.1 Wear Resistance

Wear is the removal of material from the surfaces of bodies that come into contact with each other. In general, two types of wear can be distinguished for ceramics[25]. They are, adhesive wear and abrasive wear. Adhesive wear may occur when two ceramic surfaces or a ceramic surface and a metallic surface are in contact with each other. This type of wear is the result of fracture occurring in the ceramic as a result of the tangential motion which occurs when sliding or rubbing one surface over the other.

Abrasive wear occurs when two surfaces, one considerably harder than the other, are brought into contact with each other. When free particles of these harder materials are generated and imposed at the interface between the two surfaces, these particles can cut into and remove materials from the softer surface.

TABLE 9: Slag Glass-ceramics[1,2,6,13,21,24]

Major Constituent and Concentration (wt.%)	SiO_2 (30-63), Al_2O_3 (5-30), CaO (9-47), MgO (up to 10, preferred at 5)
Nucleating Agents (Wt.%)	- Oxides of zinc, iron manganese, chromium, titanium. - Iron ores, chrome ores. - Calcium fluoride. - Heavy metal sulphides (0-15%)
Heat Treatment	- Melting : 1400 - 1600°C - Nucleation : 650 - 800°C - Crystallization: 800 - 1100°C
Crystalline Phase	Diopside, $CaMg(SiO_3)_2$[21]; Akermanite $Ca_2MgSi_2O_7$; Wollastonite, $CaSiO_3$; Anorthite, $CaAl_2Si_2O_8$; clinopyroxene, monoclinic pyroxene[24].
Physical Properties	- Density ~ 2.9 $g.cm^{-3}$ - Softening Temperature 770-1225°C - Vicker's hardness 750[21] - Moh's scale 8-8½ - Modulus of Rupture ~1400 $kg.cm^{-2}$ - Loss of Mass on Abrasion 0.179 $kg.cm^{-2}$[24] - Acid resistance (96° H_2SO_4) 98.7

Abrasive wear can also occur when a third particle harder than one or both of the surfaces in contact with each other is trapped in the interface. This particle can remove the material from one or both surfaces.

A third type of abrasive wear can result from the impingement of finely divided solids, such as silicon carbide, that are suspended in the surrounding medium of the ceramic (air, gas or liquid).

6.2 Abrasion Resistance

The degree of abrasion-resistance of a material depends upon the grain size, hardness, shape,weight and the operating conditions, such as the atmosphere, the prevailing temperature, etc. McMillan[1] suggested that the abrasion resistance of a material under closely specified conditions may be taken as one measure of its hardness. Using Moh's scale glass-ceramics may reach hardness approximating those of corundum (Al_2O_3) and silicon carbide which are in the 9-9.5 range. Glass-ceramics may reach hardness, considerably greater than those of glasses which are usually between 5 and 7.

Besides the scratch test associated with Moh's scale indentation hardness techniques such as the Knoop hardness test, the diamond pyramid hardness test (D.P.H.) and the Rockwell test can be applied although none of these methods can be regarded as truly satisfactory for measuring the hardness of non-ductile materials such as glass-ceramics.

ORF

6.3 Methods of Measurement

The abrasion resistance of glass-ceramic and ceramic can be measured by two techniques:

(a) Impingement by hard and fine solids (silicon carbide, Alumina powder, etc.) suspended in either air, gas or liquid.

(b) Direct abrasion by dry or wet solids moving across the surface.

A variety of techniques for the measurement of the abrasion resistance of glasses and other materials are known. Common methods are hand abrasion with emery cloth, diamond scratching, a grinding wheel, etc.

A new technique has been reported [26] which uses a Minimet polisher as a testing device for abrasion. A grit blaster using silicon carbide particles has also been used to evaluate the abrasion resistance of glasses and glass-ceramics[27,28].

7. FRACTURE AND CRACK INHIBITION OF GLASS-CERAMICS

7.1 Fracture of Glass

The fracture strength or the cohesive strength of a cyrstal is the force necessary to overcome the attraction exerted by an ionic crystal per unit area. It can be claculated from the following equation.

$$\sigma_{max} = \frac{f_{max}}{r_o^2}$$

...where σ_{max} : is the cohesive strength of the crystal

r_o is the distance separating two close ions

f_{max}: Is the force required to separate the ions.

Experiments have shown that the actual fracture strength of a real glass falls short of the computed value of the cohesive strength by as much as three orders of magnitude.

Griffith[29] postulated that the microcracks in glass are the main reason for the low strength of this material. Once a crack begins to grow, less force is required to spread it further. For ordinary glass[30]:

$$\sigma\sqrt{c} = 1.23 \times 10^7 \text{ (dyne/cm}^2\text{)}$$

where σ is the stress and c is the critical length of the crack.

Griffith made the assumption that invisible cracks formed during solidification of the melt.

Griffith theory is of interest because it postulates that the strength of a brittle material can be improved if the size of the crack is reduced. However, the crack size is not the only factor which determines the strength of the glass, equally important is the surface tension. If a glass is exposed to the air, the moisture and oxygen of the air are absorbed onto the surface cracks which reduces their specific surface energy, thereby lowering their mechanical strength.

7.2 Strength and Fracture Properties of Glass-ceramics

The mechanical strength of glass-ceramics is higher than those of many conventional ceramics and glasses when comparing specimens which received the same abrasion treatment. The strength of glass-ceramics can be expressed in terms of the parameters of fracture mechanics, i.e., flaw size and shape, fracture energy and elastic modulus. Except for the flaw size, the other parameters can be measured as a function of glass-ceramic microstructure.

The presence of crystals[1] in glass-ceramics and the absence of pores contribute to the high strength of these materials. Crystals in glass-ceramics cause deflection and possibly blunting of the fracture tips. Thus the load required to cause fracture is increased and the formation of cracks occurs less readily or is even halted as the applied stress traverses the boundaries between the crystalline phases. The only source of porosity in glass-ceramics is from gas bubbles formed during pouring. Pores do not develop during the conversion from the glassy to the ceramic state since the overall volume change is very small.

Y. Utsumi and S. Sakka[32] suggested that the mechanical strength of a glass-ceramic is related to the mean grain diameter d by the relationship:

$$\sigma = Kd^{1/2}$$

where K is a constant. The implication of this relationship is that the crack length in the Griffith equation is proportional to the grain diameter

$$\sigma = \left(\frac{2E\alpha}{\pi C}\right)^{1/2}$$

where E is the elastic modulus (N/m^2) and α is the fracture surface energy (J/m^2).

Freidman et.al. studied the mechanical properties of $BaO\text{-}SiO_2$ glass-ceramics[33]. They found that the strength of glass-ceramics depended on the nucleation heat treatment and that maximum strength was obtained with lathlike structures. The strength increase is attributed to the difficulty of crack propagation through randomly oriented crystals. Fracture occurs primarily transgranually in all microstructures and some cleavage planes can be seen in the lathlike structure. The abrasion resistance does not depend on the microstructure of the glass-ceramics.

Hing and McMillan[34], in a study of Li_2O-Al_2O_3-SiO_2 glass-ceramics stated that the microstructure of glass-ceramics can be quite complex and their characterization requires extensive electron microscopy studies. The complexity arises partly because the addition of minor constituents to facilitate the glass formation and crystal nucleation often alters the kinetics of glass in glass phase separation of the resulting glass-ceramics. The strength of a glass-ceramic is found to increase with the inverse of the square root of the mean free path in the intercrystalline glass phase. The overall strength of a glass-ceramic, however, is dictated more by the mechani-, cal and thermal compatibility of the precipitated phases rather than by the ed crystal size alone.

The mean free path, λ, or the average separation between crystals can be calculated from:

$$\lambda = d\ (1 - V_f)/V_f$$

where V_f is the volume of the crystalline phase and d is the mean crystal size.

Govila, et.al.[35] investigated the crack propagation mechanism in LiO_2-Al_2O_3-SiO_2 glass-ceramics as a function of both initial flaw-size and temperature. Transgranular cracks were observed up to 900°C, and above this temperature subcritical crack growth occurred intergranularly.

The degree of intergranular and transgranular fracture in polycrystalline bodies is important since it may correlate with the strength and cause failure. Cleavage or fracture steps which form the well known "river pattern" of transgranular failure can generally be followed back to the fracture origin. Fracture steps are also caused by dislocations in inhomegeneities such as pores.

ORE

Intergranular failure generally increased with test temperatures, grain boundary impurities and porosity. Since these factors also generally lower the strength, and increase in intergranular failure may indicate a reduction in the strength of the glass-ceramic. Negro and Bachiorrini[36] found that the fracture surface of glass-ceramics is essentially trans-crystalline with river cleavages. It was found that CaO increases the grain size, Al_2O_3 raises the brittleness, SiO_2 enhances the fracture propagation and MgO improves the devitrification.

7.3 Methods of Testing the Strength of Glass

The strength of a glass or a glass-ceramic, and its resistance to fracture can be investigated by bending a glass beam. A beam under load at one surface has tensile stress on one side and compressive stress on the other. Maximum stress occurs at the surface. In three point bending (Figure 6) the maximum tensile stress occurs at the central load point. In four point bending (Figure 7), the whole loading surface experiences the same maximum tensile stress. Therefore, four point bending produces a result which is more representative for the material as a whole than three point bending.

Provided that the spacing of the loading point is large compared with the depth of the beam and that the deflection of the beam is small, the maximum tensile surface stress is given by:

$$\sigma_{max} = \frac{M}{D}$$

where M is the maximum bending movement

$$M = \frac{La}{2}$$

and D depends on the dimension and the cross-section of the beam $D = \frac{1}{4}\pi r^3$ for circular cross-section, for rectangular $D = \frac{1}{6}$ width x $(\text{depth})^2$.

ORE

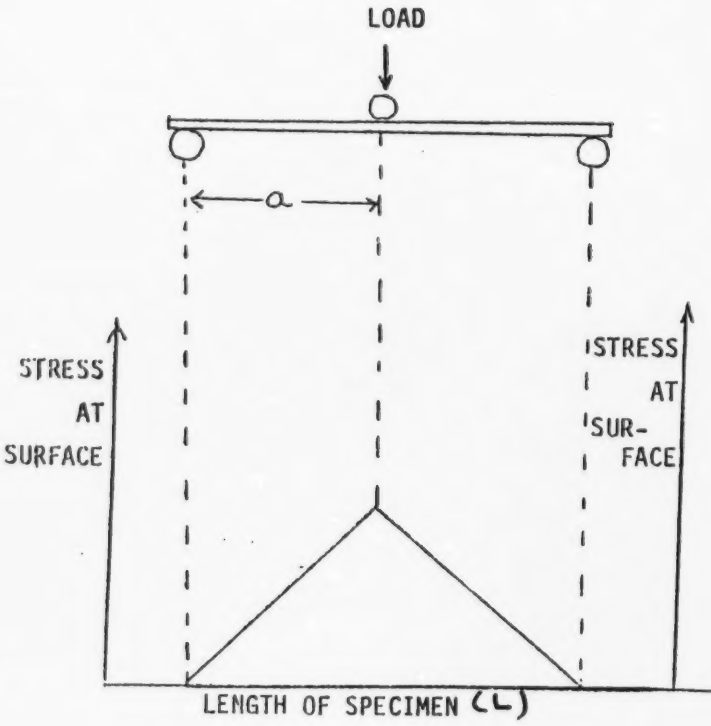

FIGURE 6: Three Point Bending

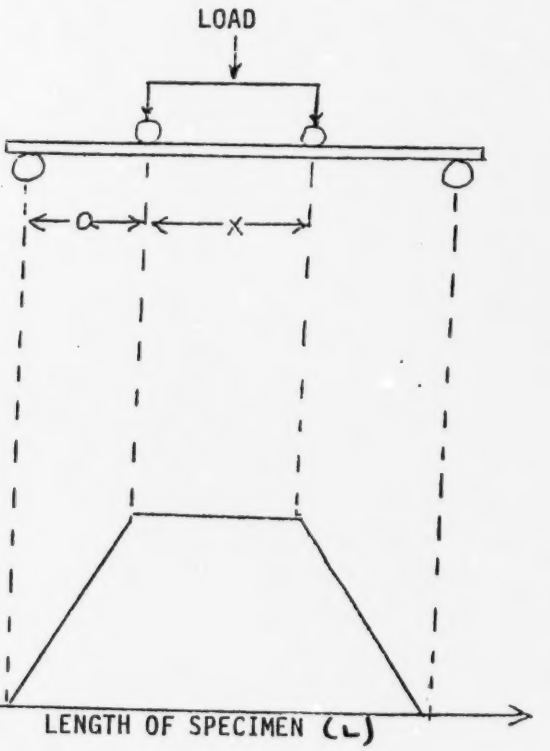

FIGURE 7: Four Point Bending

ORF

The modulus of rupture can be found by the following equation:

$$M.O.R. = \frac{3La}{bd^2}$$

where b is the width ahd d is the thickness of the specimen.

7.4 Fracture Topography Techniques[37]

The optical scanning electron (SEM) and transmission electron (TEM) microscopes are typically used for studying fracture topography.

The optical microscope remains one of the most useful and cost-effective tools. However, the optical microscope can only be used to study relatively fine microstructures since its depth of field is limited. The SEM is much more useful especially when used in conjunction with the optical microscope. It has an extremely large depth of focus and is therefore applicable to fracture studies. Resolution better than 300 A^0 has been achieved.

TEM is not capable of examining fracture directly. It is necessary to employ a replica of the fracture surface. Numerous replication procedures for transmission electron fractography have been developed. The most common methods are the plastic tape, the direct carbon and the oxide film techniques. TEM delineates the structure of fine pores better than SEM, but often fails to reveal larger features, such as large pores or cracks due to replica breakage. The Electron Microprobe Analyzer has also found application in fractography. It has the unique capability of quantitatively analyzing areas as small as 7μm in diameter for their composition. This technique can be applied to identify segregation of impurities and phases at the fracture surface.

ORF

7.5 Crack Inhibition in Glass-ceramics

Pletka and Wiederhorn[38] found that microparticles in glass-ceramics appear to block the crack motion in a magnesium alumino-silicate glass-ceramics. This type of interaction has not been found for lithium alumino-silicate glass-ceramics which have a relatively homogeneous microstructure. A crack that becomes momentarily arrested by particles will require a higher force to propagate.

It is possible[1] that the mechanical strength of glass-ceramics is controlled by the distribution of microcracks on the surface. The presence of crystals may slow down or even arrest the crack propogation as it crosses boundaries between crystalline and glass phases whereas in glasses there will be an uninterrupted path.

The length of the microcracks in glass-ceramics will be related to the size and the volume fraction of the cyrstal phases and it is probable that an optimum microstructure exists which will result in a minimum average micro-cracks length and therefore in a maximum mechanical strength. Utsumi and Sakka[32] suggested that the mechanical strength of a glass-ceramic, σ, is directly proportional to the grain diameter as shown in the equation below (also Figure 10).

$$\sigma = Kd^{-\frac{1}{2}}$$

where K is constant
d is the grain diameter

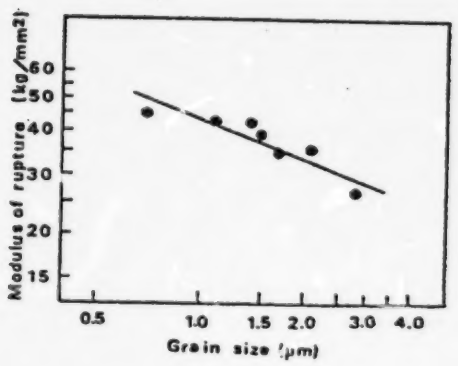

FIGURE 10: Bending strength as function of grain size for glass-ceramic after removal of surface layer. (Reference 22.)

High and McMillan[34] examined the strength of bulk crystallized glass with composition 68 SiO_2, 29 Li_2O, 1 ZnO, 1 P_2O_5, 1 K_2O. The glasses were nucleated at 500°C, then crystallized at 550°C. Bars were cut, polished and notched for the strength measurements. The major crystalline phase found was lithium disilicate. The mechanical strength of the glass-ceramics increases as the duration of the heat treatment increases, up to 24 hours, after which time the strength begins to decrease (Figure 11). Even coarse grained glass-ceramics showed significant increases in strength. The authors attribute the increased mechanical strength to several factors including subsidiary cracking of the amorphous phase, segmentation of the crack by the crystalline phase and misorientation of the crystals with respect to the fracture path with a resulting increased fracture surface area. The last concept is of particular interest, because it suggests that the randomly oriented crystals could absorb elastic energy from the advancing crack by cleavage of the crystal.

ORF

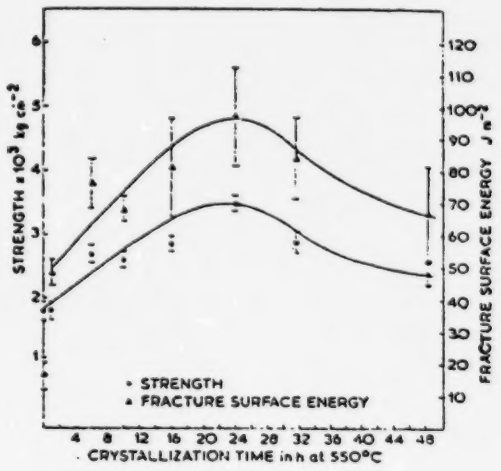

FIGURE 11: Effect of crystallization time at 550°C on the strength and fracture surface energy. All the specimens were given a nucleation heat treatment of 500°C for 1 1b. (Reference 34).

Borom, et.al.[37] evaluated the effect of microstructure on the strength of lithium disilicate glass-ceramics. Strength measurements were performed on etched and ground glass rods, in order to obtain a uniform degree of surface damage. Strength was measured with a four-point bending test after varying nucleation and crystallization schedules (Table 10). Figure 8 shows the effect of crystal growth temperature upon strength. Crystalline phases grown at temperatures below 800°C have no effect on strength. However, the formation of a $Li_2Si_2O_5$ phase above 800°C gives increasing strength with increasing growth temperature. Sample 1-13 showed a four-fold increase in strength which the authors associated with the formation of a lithium disilicate surface area. The major difference in the preparation of this sample was a much longer nucleation time (168 hours) compared to the other glasses. Microscopic examination of the fracture surfaces showed that fracture porpagated through the Li_2SiO_3 crystalline phases while $Li_2Si_2O_5$ crystalline phases deflected the cracks. The authors attributed the increase of strength caused by the lithium disilicate crystalline phases to the higher thermal expansion of the $Li_2Si_2O_5$ phase. The

difference in thermal expansion of the crystalline and glassy phases generates compressive stresses throughout the glass-ceramic. Crack propagation is inhibited because the stress fields around the crystals absorb the crack energy and inhibit crack propagation.

When $Li_2Si_2O_5$ is the only major crystalline phase, the strength increases as the size increases and the number of lithium disilicate crystals decrease.

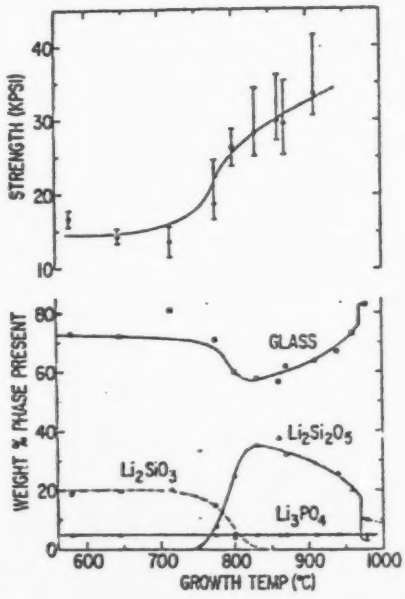

FIGURE 12: Plot showing correlation between strength and phases present as a function of growth temperature. Data, except for points at 580°C and 645°C (specimens 1-1 and 1-23) are for specimens of parent glass nucleated for 1 h at 645°C followed by 4 h at growth temperature indicated. (Reference 39).

TABLE 10: Isothermal Heat Treatments, X-Ray Results, Mechanical Strength Data, and Physical Properties.

Sample No.	Nucleation Temp. (°C)	Nucleation Time (h)	Growth Temp. (°C)	Growth Time (h)	Avg breaking strength (psi × 10^{-3})	Composition (wt%) Glass	Li_3PO_4	Meta Li_2SiO_3	Di $Li_2Si_2O_5$	E (psi × 10^{-6})	Density (g/cm³)	n_D
I-1	580	4			16.7	73	5	19	0			
I-2	"	20			13.5	68	4	20	0			
I-3	645	0.5	800	0.5	9.2	71	3	27	<1			
I-4	"	1	725	0.5	21.5*	77	4	18	0			
I-5	"	"	715	4	29.4*	81	3	20	0			
I-6	"	"	725	4	13.5	81	3	20	0	11.4	2.38	
I-7	"	"	735	36	†	81	3	5	14			
I-8	"	"	775	4	18.8	71	5	15	8			
I-9	"	"	800	0.5	10.9	68	4	22	6			
I-10	"	"	"	4	26.4	60	4	5	25			
I-11	"	"	830	0.5	20.7	63	4	<2	37			
I-12	"	"	"	4	28.2	58	5	0	35	13.0	2.40	
I-13	"	"	"	168	55.8	50	1.5	tr.	46			
I-14	"	"	860	4	30.0*	57	5	0	38			
I-15	"	"	870	"	29.6	62	5	0	32			
I-16	"	"	910	0.5	29.9*	62	5	tr.	25			
I-17	"	"	"	0.5	28.5	60	5	tr.	27			
I-18	"	"	"	4	33.6	64	5	2	29	12.5	2.40	
I-19	"	"	"	24	29.6	58	2-3.3	5	36			
I-20	"	"	940	4		67	5	4	26			
I-21	"	"	960	16		73	4	4	20			
I-22	"	"	978	8	‡	83	5	10	3			
I-23	"	18	None	None	14.2	72	5	20	tr.			
I-O	As drawn from melt				14.5	100	0	0	0	10.2	2.34	1.52
I-M	Matrix glass, as drawn from melt										2.35	1.50
$Li_2Si_2O_5$											2.44	1.55
Li_2SiO_3											2.51	1.59

*Centerless-ground before heat treatment. †Bulk specimens. ‡Rods deformed during heat treatment.

(Reference 39)

ORF

8. REFERENCES

1) McMillan, P.W., Glass-Ceramics, Ac. Press, London, 2nd ed. (1979).

2) Stookey, S.D., Chem. Eng. News, 39 (25), 116-125 (1961).

3) Tamman, G., The States of Aggregation, D. van Nostrand Co., (1925).

4) Briggs, J. and Carruthers, T.G., Phys. Chem. Glasses 17 (2), 30-35 (1976).

5) Šesták, J., Phys. Chem. Glasses 15 (6), 137-140 (1974).

6) Thaku, R.L., in Advances in Nucleation and Crystallization, Amer. Ceram. Soc., Special Publication No. 5, pp. 166-172 (1971).

7) Gutt, W., Silic. Ind. 27, 285 - (1962).

8) Pei, Y.K., German Pat. 2, 119, 771 (1971).

9) Goss, G.L., Prod. Eng. 33, 52-55 (1962).

10) Beall, G.H. and Rittler, H., U.S. Pat. 3,557,575 (1971).

11) U.S. Pat. 4,009.015 (1977).

12) Lehrke, W.D., and Nonnen, F.A., Int. Conference on the Internal and External Protection of Pipes, Univ. of Durham, U.K. (Sept. 9-11, 1975).

13) Berezhnoi, A.I., Glass-Ceramics and Photo-Sitalls, Plenum Press, New York (1970).

14) MacDowell, J.F. and Beall, G.H., J. Amer. Ceram. Soc. 52, 17-25, (1969).

15) Beall, G.H. and Rittler, H.,Ceram. Bull. 55 (6), 579-582 (1976).

16) Omar, A.A. and El-Shennawi, A.W.A., Nature Physical Science, 231, 44- (1971).

17) Davies, M.W., Kerrison, B., Gross, W.E., Robson, M.H., and Wichall, D.F., J. Iron, Steel Inst. 208, 348-370 (1970).

18) B.P. 986, 289 (1965).

19) Bondarez, "Slag Sitall - A material of the future", 9th Int. Cong. Glass (1971), p. 1237-1250.

20) Löscei, B.P., (Symposium on Nucleation and Crystallization in Glass and Metals", American Ceramic Society, (1961) p. 71-75.

21) Veasey, T.J., J. Mineral Sci., 5 (2), 92-107 (1973).

22) Diken, G.M.,Smyth, H.T., McLaren, M.G., Silic. Ind. 41, 53 - (1976).

23) Mascolo, G., Buri A., Mapotta A., Sabatelli, V., Annali di Chimica, 66, 251-260 (1976).

24) Kislitsyn, B.F., Sas, R.I., Golius, T.E., Polishchuk, N.A., Scient. Res. Inst. Automobile Glass, 1, 9-10 (Jan. 1981).

25) Buckley, D.H., Ceram. Bull 51 (12), 824-905 (1972).

26) Baranyi, A.D., "Development of Abrasion Resistant Ceramics" Final Report, Ontario Research Foundation (December 1980).

27) Mould, R.E., and Southwick, J., Amer. Ceramic Soc. 42 (12), 542-547 (1959), 43 (12), 582-592 (1959); 43 (3), 160-167 (1960).

28) Watanabe M., Caporali, R.V., Mould, R.E., "Symposium on Nucleation and Crystallization in Glasses and Melts", The American Ceramic Society (1962), pp. 23.

29) Griffith, A.A., Philo. Trans. Roy. Soc. (London) A221, 163 (1920).

30) Morey, G.W., The Property of Glass, Reinhold, N.Y. (1954).

31) Borom, M.P., Turkalo, A.M., and Doremus, R.H., J. Amer. Ceram. Soc. 58, 385-391 (1975).

32) Utsumi, Y. and Sakka, S., J. Amer. Ceram. Soc. 53, 286-287 (1970).

33) Freiman, S.W., Onoda, G.Y. and Pinaus, A.G., J. Amer. Ceram. Soc. 57 (1), 8-12 (1974).

34) Hing, P., and McMillan, P.W., J. Mat. Sci. 8, 1041-1048 (1973).

35) Govila, R.K., Kinsman, K.R., and Beardmore, P., J. Mat. Sci. 13, 2081-2091 (1978).

36) Negro, A., and Bachiorrini, A., Ceramurgia 4 (1974).

37) McCall, J.L., Symposium on Electronfractography, Boston (1967) ASTM.

38) Pletka, B.J., and Wiederhorn, S.M., Fracture Mechanics of Ceramics, Plenum Press, N.Y., 4, 745-761 (1978).

ORF

APPENDIX B

ABRASION TESTING RESULTS

OF GLASSES

ABRASION MEASUREMENT RESULTS

GLASS COMP.	SURFACE AREA ($dm^2 x 10^{-2}$)	WT OF GRIT (g)	WT BEFORE (g)	PRESSURE (PSI)	TIME (s)	WT AFTER (g)	WT LOSS (g)	$\frac{\text{WT LOSS}}{\text{SURFACE AREA}}$ ($g.dm^{-2}$)	AVG. $\frac{\text{WT LOSS}}{\text{SURFACE AREA}}$ ($g.dm^{-2}$)
1	0.785	35	4.6593	40	60	4.6535	.0058	.7389	
1	0.785	35	4.6535	40	60	4.6483	.0052	.6624	.6784
1	0.785	35	3.6871	40	60	3.6822	.0049	.6242	
1	0.785	35	3.6822	40	60	3.6768	.0054	.6879	
2	0.785	35	4.8712	40	60	4.8646	.0066	.8408	
2	0.785	35	4.8646	40	60	4.8566	.0080	1.0191	.8758
2	0.785	35	4.4604	40	60	4.4544	.0060	.7643	
2	0.785	35	4.4544	40	60	4.4475	.0049	.8790	
5	0.5024	35	4.0026	40	60	3.9965	.0061	1.2142	
5	0.5024	35	3.9965	40	60	3.9917	.0048	.9554	1.0798
5	0.5024	35	3.5534	40	60	3.5475	.0059	1.1744	
5	0.5024	35	3.5475	40	60	3.5426	.0049	.9753	

ORF

ABRASION MEASUREMENT RESULTS

GLASS COMP.	SURFACE AREA ($dm^2 x 10^{-2}$)	WT OF GRIT (g)	WT BEFORE (g)	PRESSURE (PSI)	TIME (s)	WT AFTER (g)	WT LOSS (g)	$\frac{\text{WT LOSS}}{\text{SURFACE AREA}}$ ($g.dm^{-2}$)	AVG. $\frac{\text{WT LOSS}}{\text{SURFACE AREA}}$ ($g.dm^{-2}$)
7	.5024	35	3.7456	40	60	3.7392	.0064	1.2739	1.0500
7	.5024	35	3.7392	40	60	3.7350	.0042	.8360	
7	.5024	35	4.0032	40	60	3.9980	.0052	1.0350	
7	.5024	35	3.9980	40	60	3.9927	.0053	1.0549	
7	.785	35	4.7248	40	60	4.7188	.0060	.7643	.7357
8	.785	35	4.7188	40	60	4.7131	.0057	.7261	
8	.785	35	4.6650	40	60	4.6594	.0056	.7134	
8	.785	35	4.6594	40	60	4.6536	.0058	.7389	
12	.785	35	4.8273	40	60	4.8211	.0062	.7898	.8567
12	.785	35	4.8211	40	60	4.8138	.0073	.9299	
12	.785	35	4.8724	40	60	4.8663	.0061	.7771	
12	.785	35	4.8663	40	60	4.8590	.0073	.9299	

ABRASION MEASUREMENT RESULTS

GLASS COMP.	SURFACE AREA ($dm^2 x 10^{-2}$)	WT OF GRIT (g)	WT BEFORE (g)	PRESSURE (PSI)	TIME (s)	WT AFTER (g)	WT LOSS (g)	$\frac{\text{WT LOSS}}{\text{SURFACE AREA}}$ ($g.dm^{-2}$)	AVG. $\frac{\text{WT LOSS}}{\text{SURFACE AREA}}$ ($g.dm^{-2}$)
13	.785	35	4.7306	40	60	4.7244	.0062	.7898	
13	.785	35	4.7244	40	60	4.7122	.0072	.9172	.8248
13	.785	35	4.8228	40	60	4.8166	.0062	.7898	
13	.785	35	4.8166	40	60	4.8103	.0063	.8025	
14	.785	35	4.7514	40	60	4.7451	.0063	.8025	
14	.785	35	4.7451	40	60	4.7385	.0066	.8408	.8026
14	.785	35	4.5845	40	60	4.5788	.0057	.7261	
14	.785	35	4.5788	40	60	4.5722	.0066	.8408	
15	.785	35	4.4636	40	60	4.4565	.0071	.9045	
15	.785	35	4.4565	40	60	4.4488	.0077	.9809	1.0064
15	.785	35	5.2445	40	60	5.2364	.0081	1.0318	
15	.785	35	5.2364	40	60	5.2277	.0087	1.1083	

ORF

APPENDIX C

ABRASION TESTING RESULTS OF GLASS-CERAMICS

HEAT TREATMENT

AND

ABRASION MEASUREMENT RESULTS

GLASS COMP.	NUCLEATION TEMP. (°C)	NUCLEATION TIME (HR)	CRYSTALLIZATION TEMP. (°C)	CRYSTALLIZATION TIME (HR)	SURFACE AREA ($dm^2 x 10^{-2}$)	WT OF GRIT (g)	WT BEFORE (g)	PRESSURE (PSI)	TIME (s)	WT AFTER (g)	WT Loss (g)	WT LOSS / SURFACE AREA ($g.dm^{-2}$)	AVG. WT LOSS / SURFACE AREA ($g.dm^{-2}$)
Alumina	-	-	-	-	0.785	35	7.3476	40	60	7.3472	.0004	.0510	.0446
Alumina	-	-	-	-	0.785	35	7.3472	40	60	7.3469	.0003	.0382	
1	840	6	950	24	0.785	35	3.6045	40	60	3.6012	.0033	.4204	.3609
1	840	6	950	24	0.785	35	4.5390	40	60	4.5365	.0025	.3185	
1	840	6	950	24	0.785	35	4.5365	40	60	4.5338	.0027	.3439	
1	860	12	960	24	0.785	35	3.7868	40	60	3.7819	.0049	.6242	.6306
1	860	12	960	24	0.785	35	3.7819	40	60	3.7769	.0050	.6369	
1	900	24	1000	24	0.785	35	5.2957	40	60	5.2928	.0029	.3694	.4363
1	900	24	1000	26	0.785	35	5.2928	40	60	5.2880	.0048	.6115	
1	900	24	1000	24	0.785	35	4.6677	40	60	4.6646	.0031	.3949	
1	900	24	1000	24	0.785	35	4.6646	40	60	4.6617	.0029	.3694	
1	950	24	1050	26	0.785	35	5.9618	40	60	5.9582	.0036	.4586	.4395
1	950	24	1050	26	0.785	35	5.9548	40	60	5.9544	.0034	.4331	
1	950	24	1050	26	0.785	35	5.1006	40	60	5.0964	.0042	.5350	

ORF

HEAT TREATMENT

AND

ABRASION MEASUREMENT RESULTS

GLASS COMP.	NUCLEATION TEMP. (°C)	NUCLEATION TIME (HR)	CRYSTALLIZATION TEMP. (°C)	CRYSTALLIZATION TIME (HR)	SURFACE AREA ($dm^2 x 10^{-2}$)	WT OF GRIT (g)	WT BEFORE (g)	PRESSURE (PSI)	TIME (s)	WT AFTER (g)	WT Loss (g)	WT LOSS / SURFACE AREA$_2$ ($g.dm^{-2}$)	AVG. WT LOSS / SURFACE AREA$_2$ ($g.dm^{-2}$)
1	950	24	1050	24	0.785	35	5.0964	40	60	5.0938	.0026	.3312	
2	730	24	900	24	0.785	35	5.6095	40	60	5.6046	.0049	.6242	.6816
2	730	24	900	24	0.785	35	4.6839	40	60	4.6781	.0058	.7389	
2	800	12	830	24	0.5024	35	4.8055	40	60	4.8020	.0035	.6967	
2	800	12	830	24	0.5024	35	4.8020	40	60	4.7988	.0032	.6369	.6071
2	800	12	830	24	0.5024	35	5.0706	40	60	5.0677	.0029	.5772	
2	800	12	830	24	0.5024	35	5.0677	40	60	5.0651	.0026	.5175	
2	800	4	830	24	0.5024	35	4.5963	40	60	4.5943	.0020	.3981	
2	800	6	830	26	0.5024	35	4.5943	40	60	4.5916	.0027	.5374	.4180
2	800	6	830	26	0.5024	35	4.2947	40	60	4.2929	.0018	.3583	
2	800	6	830	26	0.5024	35	4.2929	40	60	4.2910	.0019	.3782	
2	850	4	950	24	0.785	35	5.1364	40	60	5.1324	.0040	.5096	
2	850	4	950	24	0.785	35	4.5924	40	60	4.5938	.0036	.4580	.5011
2	850	4	950	24	0.785	35	4.5938	40	60	4.5896	.0042	.5350	

HEAT TREATMENT

AND

ABRASION MEASUREMENT RESULTS

GLASS COMP.	NUCLEATION TEMP. (°C)	NUCLEATION TIME (HR)	CRYSTALLIZATION TEMP. (°C)	CRYSTALLIZATION TIME (HR)	SURFACE AREA ($dm^2 \times 10^{-2}$)	WT OF GRIT (g)	WT BEFORE (g)	PRESSURE (PSI)	TIME (s)	WT AFTER (g)	WT Loss (g)	$\frac{\text{WT LOSS}}{\text{SURFACE AREA}_2}$ ($g.dm^{-2}$)	AVG. $\frac{\text{WT LOSS}}{\text{SURFACE AREA}_2}$ ($g.dm^{-2}$)
51	750	19	850	24	0.785	35	5.2344	40	60	5.2261	.0083	1.0573	.9554
51	750	19	850	24	0.785	35	5.2261	40	60	5.2194	.0067	.8535	
52	900	17	950	24	0.785	35	6.4865	40	60	6.4836	.0029	.3694	.4522
52	900	17	950	24	0.785	35	6.4836	40	60	6.4794	.0042	.5350	
56	750	24	800	24	0.785	35	4.0053	40	60	3.9992	.0061	.7771	0.7584
56	750	24	800	24	0.785	35	3.9992	40	60	3.9918	.0074	.9427	
56	750	24	800	24	0.5024	35	3.4538	40	60	3.4513	.0025	.4976	
56	750	24	800	24	0.5024	35	3.4513	40	60	3.4472	.0041	.8161	
55b	810	4	910	14	0.785	35	4.3252	40	60	4.3174	.0078	.9936	.8280
55b	810	4	910	14	0.785	35	4.3174	40	60	4.3123	.0051	.6497	
55b	810	4	910	14	0.785	35	4.8029	40	60	4.7963	.0066	.8408	

ORF

HEAT TREATMENT AND ABRASION MEASUREMENT RESULTS

GLASS COMP.	NUCLEATION TEMP. (°C)	NUCLEATION TIME (HR)	CRYSTALLIZATION TEMP. (°C)	CRYSTALLIZATION TIME (HR)	SURFACE AREA ($dm^2 \times 10^{-2}$)	WT OF GRIT (g)	WT BEFORE (g)	PRESSURE (PSI)	TIME (s)	WT AFTER (g)	WT Loss (g)	$\frac{\text{WT LOSS}}{\text{SURFACE AREA}_2}$ ($g.dm^{-2}$)	AVG. $\frac{\text{WT LOSS}}{\text{SURFACE AREA}_2}$ ($g.dm^{-2}$)
6	800	4	1000	20	0.785	35	5.4459	40	60	5.4430	0.0029	0.3694	0.6433
6	800	4	1000	20	0.785	35	5.4430	40	60	5.4358	0.0072	0.9172	
6	730	24	900	24	0.785	35	6.4747	40	60	6.4733	0.0014	0.1783	0.4012
6	730	24	900	24	0.785	35	6.4733	40	60	6.4684	0.0049	0.6242	
6	800	24	860	24	0.785	35	7.0230	40	60	7.0164	0.0066	0.8407	1.0350
6	800	24	860	24	0.785	35	6.8760	40	60	6.8664	0.0096	1.2229	
6	800	24	860	24	0.785	35	5.0569	40	60	5.0504	0.0065	0.8280	
6	800	24	860	24	0.785	35	5.0504	40	60	5.0406	0.0098	1.2489	
6	820	10	880	24	0.785	35	5.6060	40	60	5.6020	0.0040	0.5095	0.5382
6	820	10	880	24	0.785	35	5.5862	40	60	5.5811	0.0051	0.6497	
6	820	10	880	24	0.785	35	4.5150	40	60	4.5125	0.0025	0.3185	
6	820	10	880	24	0.785	35	4.5125	40	60	4.5072	0.0053	0.6751	

HEAT TREATMENT

AND

ABRASION MEASUREMENT RESULTS

GLASS COMP.	NUCLEATION TEMP. (°C)	NUCLEATION TIME (HR)	CRYSTALLIZATION TEMP. (°C)	CRYSTALLIZATION TIME (HR)	SURFACE AREA ($dm^2 \times 10^{-2}$)	WT OF GRIT (g)	WT BEFORE (g)	PRESSURE (PSI)	TIME (s)	WT AFTER (g)	WT Loss (g)	$\frac{\text{WT LOSS}}{\text{SURFACE AREA}_2}$ ($g.dm^{-2}$)	AVG. $\frac{\text{WT LOSS}}{\text{SURFACE AREA}_2}$ ($g.dm^{-2}$)
7	730	24	900	24	0.5024	35	4.9554	40	40	4.9520	0.0034	.6767	.6568
7	730	24	900	24	0.5024	35	4.9520	40	60	4.9492	0.028	.5573	
7	730	24	900	24	0.5024	35	4.7690	40	60	4.7652	0.0038	.7564	
7	730	24	900	24	0.5024	35	4.7652	40	60	4.7620	0.0032	.6369	
7	800	12	830	24	0.5024	35	4.3904	40	60	4.3876	0.0028	.5573	.5573
7	800	12	830	24	0.5024	35	4.3876	40	60	4.3857	0.0019	.3782	
7	800	12	830	24	0.5024	35	5.4119	40	60	5.4080	0.0039	.7763	
7	800	12	830	24	0.5024	35	5.4080	40	60	5.4054	0.0026	.5175	
7	850	24	950	12	0.785	35	4.7940	40	60	4.7888	0.0052	.6624	.5032
7	850	24	950	12	0.785	35	4.7888	40	60	4.7874	0.0014	0.1783	
7	850	24	950	12	0.785	35	4.2164	40	60	4.2126	0.0038	0.4841	
7	850	24	950	12	0.785	35	4.2126	40	60	4.2072	0.0054	0.6879	

ORF

HEAT TREATMENT

AND

ABRASION MEASUREMENT RESULTS

GLASS COMP.	NUCLEATION TEMP. (°C)	NUCLEATION TIME (HR)	CRYSTALLIZATION TEMP. (°C)	CRYSTALLIZATION TIME (HR)	SURFACE AREA ($dm^2 x 10^{-2}$)	WT OF GRIT (g)	WT BEFORE (g)	PRESSURE (PSI)	TIME (s)	WT AFTER (g)	WT Loss (g)	WT LOSS / SURFACE AREA ($g.dm^{-2}$)	AVG. WT LOSS / SURFACE AREA ($g.dm^{-2}$)
7	800	4	830	24	0.785	35	3.2552	40	60	3.2514	.0038	.4840	
7	800	4	830	24	0.785	35	3.2514	40	60	3.2470	0.044	.5605	.5860
7	800	4	830	24	0.785	35	3.4638	40	60	3.4575	0.063	.8025	
7	800	4	830	24	0.785	35	3.4575	40	60	3.4536	0.0390	.4968	
7	900	24	950	24	0.785	35	5.1632	40	60	5.1594	0.038	.4840	
7	900	24	950	24	0.785	35	5.1594	40	60	5.1565	0.0029	.3694	.6273
7	900	24	950	24	0.785	35	5.3992	40	60	5.3919	0.0073	.9299	
7	900	24	950	24	0.785	35	5.3919	40	60	5.3862	0.0057	.7261	
7	850	4	950	24	0.785	35	6.5347	40	60	6.5333	0.0014	.1783	
7	850	4	950	24	0.785	35	6.5333	40	60	6.5318	0.0015	.1910	.2451
7	850	4	950	24	0.785	35	5.4350	40	60	5.4314	0.0036	.4586	
7	850	4	950	24	0.785	35	5.4314	40	60	5.4302	0.0012	.1528	

ORF

HEAT TREATMENT

AND

ABRASION MEASUREMENT RESULTS

GLASS COMP.	NUCLEATION TEMP. (°C)	NUCLEATION TIME (HR)	CRYSTALLIZATION TEMP. (°C)	CRYSTALLIZATION TIME (HR)	SURFACE AREA ($dm^2 x 10^{-2}$)	WT OF GRIT (g)	WT BEFORE (g)	PRESSURE (PSI)	TIME (s)	WT AFTER (g)	WT Loss (g)	$\frac{\text{WT LOSS}}{\text{SURFACE AREA}_2}$ ($g.dm^{-2}$)	AVG. $\frac{\text{WT LOSS}}{\text{SURFACE AREA}_2}$ ($g.dm^{-2}$)
8	800	27	900	65	0.785	35	3.5890	40	60	3.5772	0.0118		
8	800	27	900	65	0.785	35	3.5772	40	60	3.5724	0.0048	.6114	
8	800	27	900	65	0.785	35	3.282	40	60	3.2787	0.0095	1.2102	0.828
8	800	27	900	65	0.785	35	3.2787	40	60	3.2735	0.0052	.6624	
8	850	12	950	24	0.785	35	5.1460	40	60	5.1415	0.0100		
8	850	12	950	24	0.785	35	5.1415	40	60	5.1360	0.0055	.7006	
8	850	12	950	24	0.785	35	4.3935	40	60	4.3872	.0063	.8025	.7133
8	850	12	950	24	0.785	35	4.3872	40	60	4.3822	.0050	.6369	
8	850	24	950	12	0.785	35	4.2552	40	60	4.2519	.0033	.4204	
8	850	24	950	12	0.785	35	4.2519	40	60	4.2470	.0049	.6242	
8	850	24	950	12	0.785	35	3.7889	40	60	3.7839	.0050	.6370	.5924
8	850	24	950	12	0.785	35	3.7839	40	60	3.7785	.0054	.6879	
8	850	24	950	24	0.785	35	3.9141	40	60	3.9094	.0047	.5987	
8	850	24	950	24	0.785	35	3.9823	40	60	3.9765	.0058	.7388	

ORF

HEAT TREATMENT AND ABRASION MEASUREMENT RESULTS

GLASS COMP.	NUCLEATION TEMP. (°C)	NUCLEATION TIME (HR)	CRYSTALLIZATION TEMP. (°C)	CRYSTALLIZATION TIME (HR)	SURFACE AREA ($dm^2 \times 10^{-2}$)	WT OF GRIT (g)	WT BEFORE (g)	PRESSURE (PSI)	TIME (s)	WT AFTER (g)	WT Loss (g)	$\frac{\text{WT LOSS}}{\text{SURFACE AREA}_2}$ ($g.dm^{-2}$)	AVG. $\frac{\text{WT LOSS}}{\text{SURFACE AREA}_2}$ ($g.dm^{-2}$)
8	850	24	950	24	0.785	35	2.1335	40	60	2.1272	.0083	1.0573	0.7738
8	850	24	950	24	0.785	35	2.1272	40	60	2.1217	0.0055	.7006	
8	900	24	950	24	0.785	35	4.5440	40	60	4.5388	.0052	.6624	0.6497
8	900	24	950	24	0.785	35	4.1414	40	60	4.1368	.0046	.5860	
8	850	4	950	24	0.785	35	4.1368	40	60	4.1308	.0060	.7643	
8	850	4	950	24	0.785	35	3.7673	40	60	3.7628	0.0045	.5732	0.5828
8	850	4	950	24	0.785	35	3.7628	40	60	3.7586	.0042	.5350	
8	850	4	950	24	0.785	35	4.7369	40	60	4.7320	.0049	.6242	
8	850	4	950	24	0.785	35	4 .7320	40	60	4.7273	.0047	.5987	

ORF

HEAT TREATMENT

AND

ABRASION MEASUREMENT RESULTS

GLASS COMP.	NUCLEATION TEMP. (°C)	NUCLEATION TIME (HR)	CRYSTALLIZATION TEMP. (°C)	CRYSTALLIZATION TIME (HR)	SURFACE AREA ($dm^2 x 10^{-2}$)	WT OF GRIT (g)	WT BEFORE (g)	PRESSURE (PSI)	TIME (s)	WT AFTER (g)	WT Loss (g)	$\frac{\text{WT LOSS}}{\text{SURFACE AREA}_2}$ ($g.dm^{-2}$)	AVG. $\frac{\text{WT LOSS}}{\text{SURFACE AREA}_2}$ ($g.dm^{-2}$)
13	850	24	950	24	0.785	35	5.5579	40	60	5.5430	.0149	1.8981	chipped
13	850	24	950	24	0.785	35	5.5430	40	60	5.5391	.0039	.4968	.4968
13	850	24	950	12	0.785	35	5.0141	40	60	5.0105	.0036	.4586	.5287
13	850	24	950	12	0.785	35	5.0105	40	60	5.0058	.0047	.5987	
13	850	12	950	24	0.785	35	5.2204	40	60	5.2174	.0030	.3822	.4873
13	850	12	950	24	0.785	35	5.2174	40	60	5.2126	.0048	.6115	
13	850	12	950	24	0.785	35	4.8911	40	60	4.8875	.0036	.4586	
13	850	12	950	24	0.785	35	4.8875	40	60	4.8836	.0039	.4968	
13	800	27	900	65	0.785	35	4.0537	40	60	4.0506	.0031	.3949	.4650
13	800	27	900	65	0.785	35	4.0506	40	60	4.0464	.0042	.5350	
13	900	24	950	24	0.785	35	4.3491	40	60	4.3460	.0031	.3949	.3822
13	900	24	950	24	0.785	35	4.3460	40	60	4.3432	.0028	.3567	
13	900	24	950	24	0.785	35	3.1539	40	60	3.1512	.0027	.3439	
13	900	24	950	24	0.785	35	3.1512	40	60	3.1478	.0034	.4331	

ORI

HEAT TREATMENT AND ABRASION MEASUREMENT RESULTS

GLASS COMP.	NUCLEATION TEMP. (°C)	NUCLEATION TIME (HR)	CRYSTALLIZATION TEMP. (°C)	CRYSTALLIZATION TIME (HR)	SURFACE AREA ($dm^2 \times 10^{-2}$)	WT OF GRIT (g)	WT BEFORE (g)	PRESSURE (PSI)	TIME (s)	WT AFTER (g)	WT Loss (g)	WT LOSS / SURFACE AREA ($g.dm^{-2}$)	AVG. WT LOSS / SURFACE AREA ($g.dm^{-2}$)
13	850	4	950	24	0.785	35	4.0715	40	60	4.0677	.0038	.4841	
13	850	4	950	24	0.785	35	4.0677	40	60	4.0644	.0033	.4204	.4204
13	850	4	950	24	0.785	35	4.5778	40	60	4.5747	.0031	.3949	
13	850	4	950	24	0.785	35	4.5747	40	60	4.5717	.0030	.3822	
14	850	24	950	24	0.5024	35	4.0971	40	60	4.0958	.0013	.2588	
14	850	24	950	24	0.5024	35	4.0958	40	60	4.0938	.0020	.3981	.3036
14	850	24	950	24	0.5024	35	3.0160	40	60	3.0150	.0010	.1990	
14	850	24	950	24	0.5024	35	3.0150	40	60	3.0132	.0018	.3583	
14	800	27	900	65	0.785	35	4.3082	40	60	4.3036	.0046	.5860	
14	800	27	900	65	0.785	35	4.3036	40	60	4.2916	.0120	1.5287 ← chipped	
14	800	27	900	65	0.785	35	3.2460	40	60	3.2413	.0047	.5987	.7813
14	800	27	900	65	0.785	35	3.2413	40	60	3.2322	.0091	1.1592	
15	850	24	950	24	0.785	35	3.6433	40	60	3.6378	.0055	.7006	
15	850	24	950	24	0.785	35	3.6180	40	60	3.6164	.0016	.2038	.4522

ONTARIO RESEARCH FOUNDATION

ENERGY

energy conservation programs and analysis, thermal insulation design and evaluation, waste heat recovery, building energy systems and monitoring, heat storage systems, thermoelectric generation, combustion technology, burner development, heat transfer analysis, solar systems monitoring, National Solar Test Facility, solar technology, wind power, coal and lignite processing, alternate fuel utilization, battery technology, energy and chemicals from biomass, . . .

ENVIRONMENT

ambient air quality assessment, source sampling, odour emission and control, asbestos measurement and control, pesticide residues, trace metal analysis, trace organic analysis, mutagenic testing, occupational health surveys and assessments, water surveys, water purification, municipal and industrial waste water treatment processes, membrane separation techniques, wet oxidation, diesel emission control technology, solid waste treatment and recovery, noise and vibration analysis, environmental impact assessments, long-range transport of atmospheric pollutants, radiation measurements, particulate identification and measurement, ergonomics and industrial design, air pollution control technology, hazardous and toxic materials and waste control, . . .

MATERIALS

building materials, plastics, coatings and composites, metals, glass and ceramics, wood and wood composites, biomaterials, adhesives and printing inks, yarns, fabrics and geotextiles, leather, organic and inorganic chemicals, specialty formulations, specification development, quality control, mechanical chemical and thermal properties, test method development, failure analysis, fire and flammability, glass-metal seals, metal and alloy powders, metallography, materials characterization by electron microscopy and X-ray microanalysis, photovoltaics and ionic conductors, corrosion properties and control, rubber technology, energy radiography, non-destructive testing, X-ray analysis, cement and concrete, gypsum, . . .

PRODUCTS & PROCESSES

pulp and paper products, clothing, footwear and industrial textile products, knitting technology, thin and thick film systems, electronic devices, microcomputer systems and applications, fibre optics, electronic design, bioengineering, ultrasonic and fluid shear devices, microwave drying, transportation and equipment testing, mathematical stress and vibration analysis, product, equipment and machinery design and development, fuel emulsification, chemistry of foodstuffs, pulping and papermaking processes, ceramics processing, metallurgical process development, powder metal technology, packaging applications, technical and economic evaluations, industrial engineering applications, electroplating, radioactive decontamination, process control, biotechnology, industrial microbiology, enzyme analysis, cryogenics, electrical testing, . . .

RESOURCES

mineral processing, hydro and pyrometallurgical processing of ferrous and non-ferrous ores, coal evaluation and processing, asbestos processing and applications, uranium processing, forest utilization, utilization of forest and agricultural wastes, utilization of industrial mining and domestic wastes, energy and chemicals from biomass, non-metallic minerals, . . .

ONTARIO RESEARCH FOUNDATION • SHERIDAN PARK, MISSISSAUGA, ONTARIO, CANADA L5K 1B3 • (416) 822-4111 • TELEX 06-982311